RANGE AND STRAGGLING MEASUREMENTS OF U^{235} FISSION FRAGMENTS

RANGE AND STRAGGLING MEASUREMENTS OF U^{235} FISSION FRAGMENTS

By

JOHN WILLIAM HALLAM, B.Sc.

A Thesis

Submitted to the Faculty of Graduate Studies

in Partial Fulfilment of the Requirements

for the Degree

Master of Science

McMaster University

October, 1961

MASTER OF SCIENCE (1961) McMASTER UNIVERSITY
(Physics) Hamilton, Ontario

TITLE: Range and Straggling Measurements of U^{235} Fission Fragments

AUTHOR: John William Hallam, B.Sc., A.R.C.S.
(University of London)

SUPERVISOR: Dr. T. J. Kennett

NUMBER OF PAGES: viii, 67

SCOPE AND CONTENTS:

The ranges and stragglings of fission fragments from the thermal neutron fission of U^{235} have been measured. Particular attention was given to the preparation of very thin uranium sources, the design of a well collimated recoil system and the preparation of the fragment catcher. The ranges and range distributions in aluminium of fission products of mass numbers 95, 140, 141 and 147 have been obtained. The range values obtained agree with previous determinations within the experimental error. The refined techniques developed in this work have enabled differential range distributions to be obtained which are more precise than any previous determinations.

ACKNOWLEDGMENTS

I am greatly indebted to Dr. T. J. Kennett for his encouragement and guidance throughout the course of this investigation.

I should like to express my thanks to Dr. W. H. Fleming, Reactor Superintendent and to the reactor staff for their accomodating help with the irradiations. My gratitude is also expressed to Dr. K. Fritze for many helpful suggestions and discussions involving this work.

Financial assistance from McMaster University has made possible the execution and completion of this work and is gratefully acknowledged. To my wife I express my sincere thanks for help with the typing of the thesis.

TABLE OF CONTENTS

TABLE OF CONTENTS (continued)

LIST OF ILLUSTRATIONS

INTRODUCTION

1.1 General: The Fission Process

The discovery of the phenomenon known as fission was made by Hahn and Strassmann (1) in 1938. Fission may be described as the splitting of a heavy nucleus into two fragments of comparable mass. Fission can be induced by a relatively small amount of energy which may be brought into the nucleus by neutron, γ ray or charged particle capture. The process may also proceed spontaneously by a tunnelling mechanism.

The main features of the fission process are perhaps most clearly seen by means of the graphical representation shown in Fig. 1.

In the case of thermal neutron fission, a compound nucleus is formed, which decays within about 10^{-14} sec. Once the separation of the fission fragments is greater than the range of nuclear forces, the fragments are repelled from each other by the coulomb force. The fragments achieve their maximum velocity within about 10^{-17} sec after decay of the compound nucleus.

The total energy release per fission is of the order of 200 Mev. Most of this energy, about 80 percent, is in the form of kinetic energy of the fragments. The

Figure 1 is a graphic representation of the fission process. The events are:

0 Excitation of nucleus; formation of compound nucleus.

1 Fission; the fragments begin to separate.

2 Well within the electronic cloud, the fragments acquire 90 percent of their maximum kinetic energy.

3 Emission of "prompt" neutrons.

4 Emission of "prompt" γ rays.

5 The fragments, having been slowed down by the stopping material, come to rest.

The horizontal scale indicates the duration of the processes on a logarithmic scale. The vertical distances show the separation of the fragments also on a logarithmic scale. ρ is the density of the stopping material.

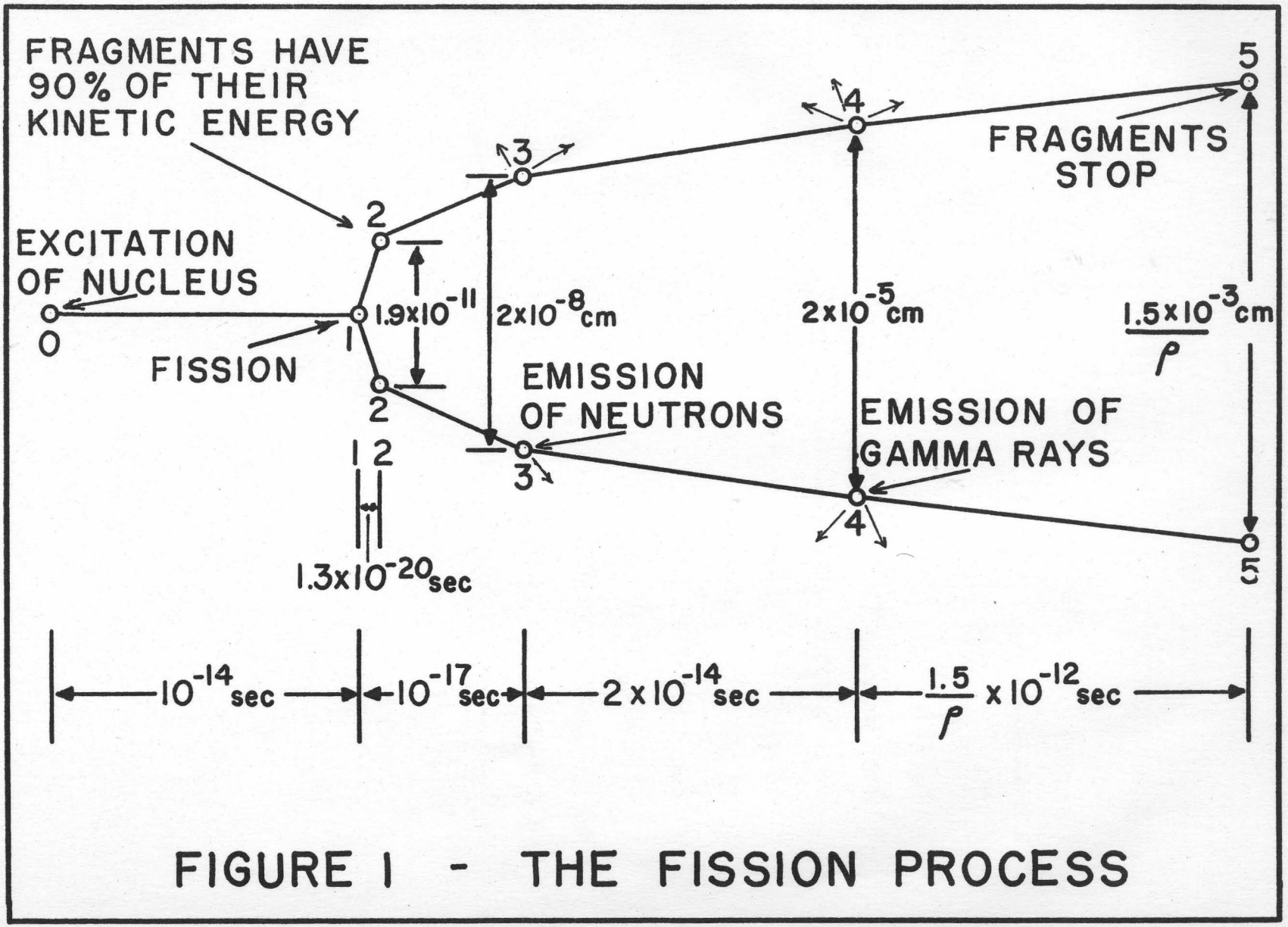

FIGURE 1 - THE FISSION PROCESS

fragments are of course in highly excited nuclear states. In fact, both fragment nuclei probably have sufficient excitation energy to boil off a neutron or two. Further deexcitation takes place by the emission of "prompt" rays. The resulting fission products still have a large neutron excess which makes them active. The subsequent and radiations are useful in many determinations since self indication techniques can be used. This technique has often been used in range determinations.

The kinetic energy spectrum of fission fragments has been investigated by various workers. The results of Brunton and Hanna (2) and Stein (3) are typical, and have been reproduced in Fig. 2. The double peaked distribution reflects the tendency of U^{235} fission fragments to be formed asymmetrically. That is to say, the probability of formation of fragments with mass numbers 88 to 100 and 135 to 145 is greater than for all other masses. The energy dispersion associated with a particular mass split is of the order of 10 percent.

The maximum velocity attained by a typical light fragment is about 1.4×10^9 cm/sec, while that of the heavier fragment is about 10^9 cm/sec. The momenta of the fragments are of course equal and opposite. The fragments attain their maximum velocity at a separation of only about 10^{-11} cm, which is well within the innermost electronic

Figure 2 shows the distribution in kinetic energy of the fragments from the slow neutron induced fission of U^{235}. The double peaked appearance is a consequence of the greater probability of assymmetric fission in this case. The results of Stein (3) have been drawn in from his time-of-flight measurements. Those of Brunton and Hanna (2) are from ionization chamber measurements and appear different from the results of Stein because of the ionization defect inherent in ionization chamber measurements of fission fragment energies.

ENERGY DISTRIBUTIONS OF SINGLE FRAGMENTS-U235

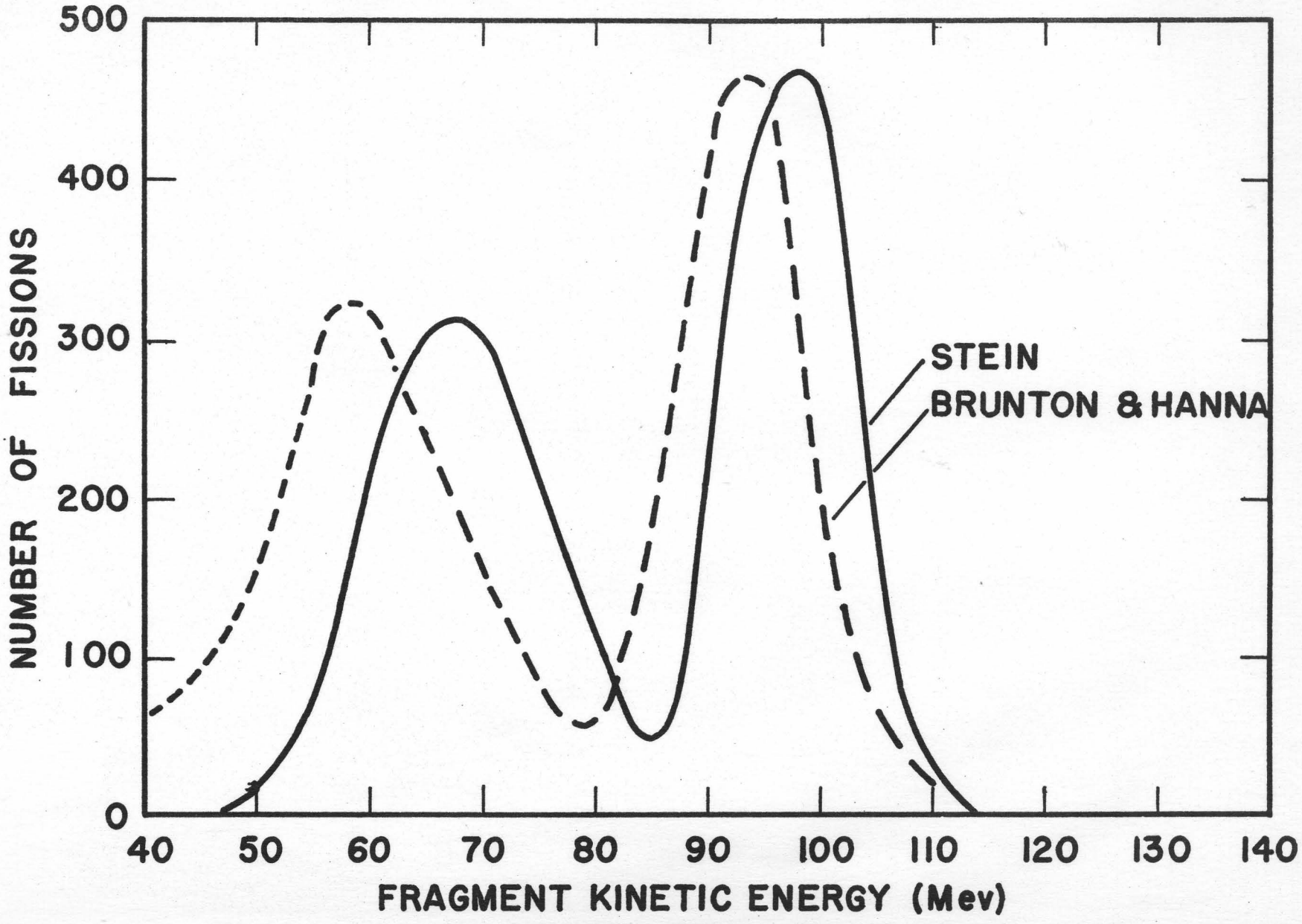

FIGURE 2

shell surrounding the fissioning nucleus.

The violence with which the fragments recoil from each other results in many of the original atomic electrons being lost. Thus the two fragments recoil from each other as ions stripped of a number of electrons. The high initial charge (~20e) on a fragment makes it more intensely ionizing than protons or alpha particles. This leads to a relatively greater rate of energy loss and to differences in the stopping mechanisms from that observed for either protons or alpha particles.

1.2 The Slowing Down and Stopping of Fission Fragments in Matter

a. General

The calculation of the interaction of fission fragments with matter is a complex problem, as can be seen by considering the processes involved in only moderate detail. Immediately after scission, the fragments have high velocities and high net charges of perhaps 20e. As a consequence of this, the fragments have very great ionizing power, enabling them to excite and ionize those atoms lying in or close to their paths. As the fragment is slowed down, its net charge decreases and thus it becomes less strongly ionizing. This is shown in Fig. 3, in which the experimental results of Lassen (4) and the theory of Bohr (5) have been incorporated. For comparison, the rate of loss of energy of a typical

Figure 3 shows comparative rate of energy loss curves for heavy and light fission fragments and alpha particles. It can be seen that the fission fragments lose energy very quickly at the beginning of their range, whereas alpha particles lose energy most rapidly just before the end of their range.

The data for the Radium C alpha particles has been taken from Henderson (1921) (6), in which the relative rate of energy loss of alpha particles is plotted versus the range in air at N.T.P.

The data for the fission fragment curves has been taken from the experimental points of Lassen (4) and the Bohr (5) energy loss formula. The graph shows the fission fragment energy loss in MeV/cm hydrogen at N.T.P.

COMPARATIVE ENERGY LOSS CURVES

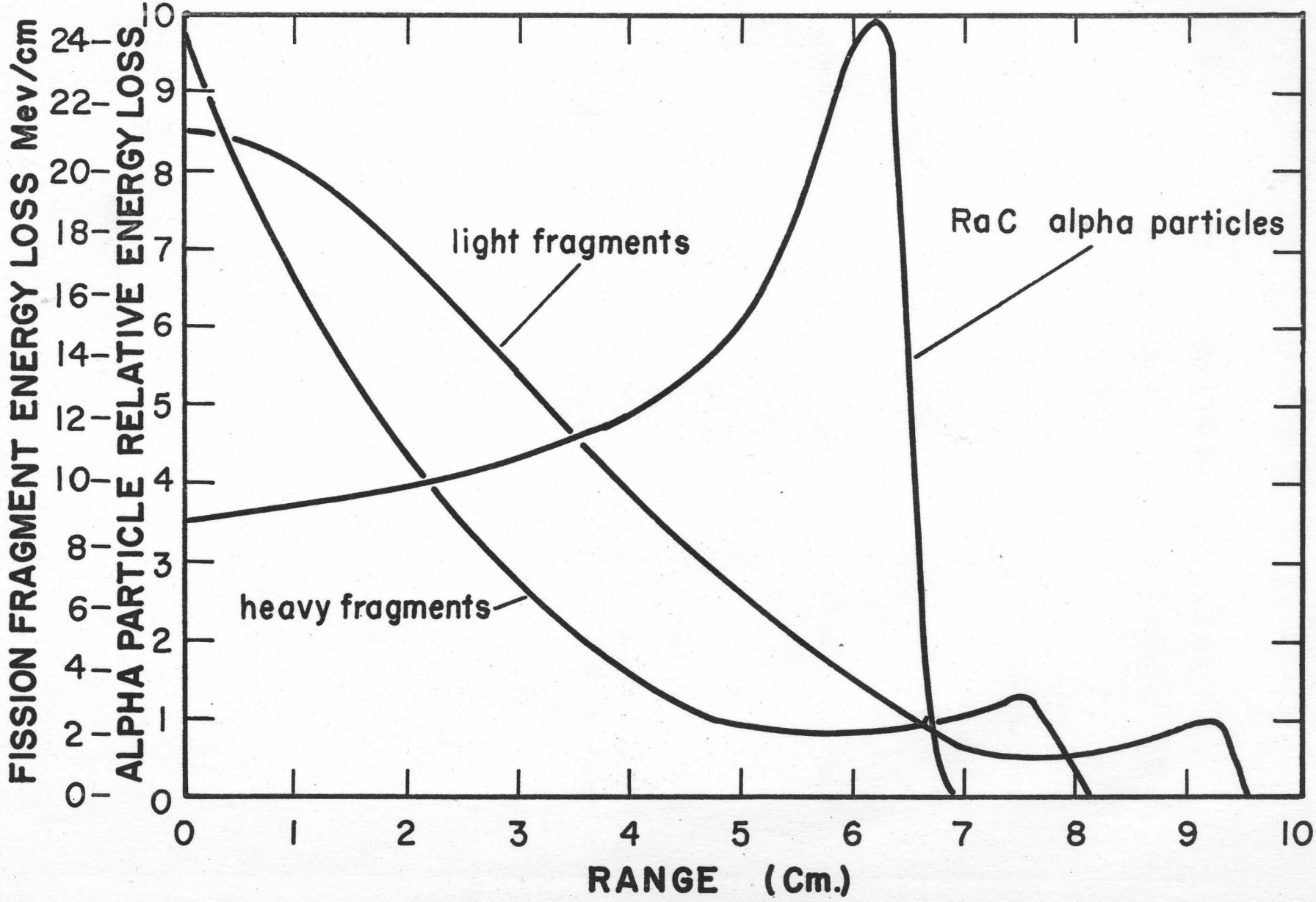

FIGURE 3

alpha particle has also been illustrated. It is seen, that in contrast to alpha particles, fission fragments lose energy most rapidly at the beginning of their ranges.

Occasionally there are atomic collisions between fragments and the atoms of the stopping material. These are the so-called "nuclear" or atomic collisions which result in relatively large energy transfer and large angle scattering. The close collision is a complex process in which both atomic and nuclear forces exert their influence to produce a rearrangement of the electronic systems of the two atoms involved.

The variation in net charge on a fragment and the occurrence of "nuclear" collisions make it very difficult to treat the slowing down process analytically.

The energy spread of fission fragments, the occurrence of large angle scattering and the charge fluctuation along the range, lead to an appreciable "straggling" or "spread in range" of a given species (Z,A) of fission fragments. The straggling of heavy, median and light fission fragments is illustrated in Fig. 4. The results of Katcoff et al, (1948) (7) have been used for this figure. The 12 - 15 percent straggling of the fission fragment species is contrasted with the relatively low 2 percent straggling of alpha particles. The lower effective charge on alpha particles results in the "nuclear" scattering of alpha particles being much smaller than for fission fragments.

Figure 4 shows a comparison of the differential range curves of three typical fission fragment species with that of the Po^{210} alpha particles. The ordinates represent the relative numbers of particles stopping after travelling through a given distance in air represented by the absisca. A range value R is shown as well as the full width at half maximum dR. The quantity dR/R x 100 is known as the percent straggling. The percent straggling of the fission fragments is between 12 and 15 percent whereas that of the alpha particles is only 2.5 percent. The fission fragment data have been drawn in from the results of Katcoff, Miskel and Stanley (1948) (7) and the alpha particle distribution has been adopted from the early work of Raynton and Wilkins (1937) (10).

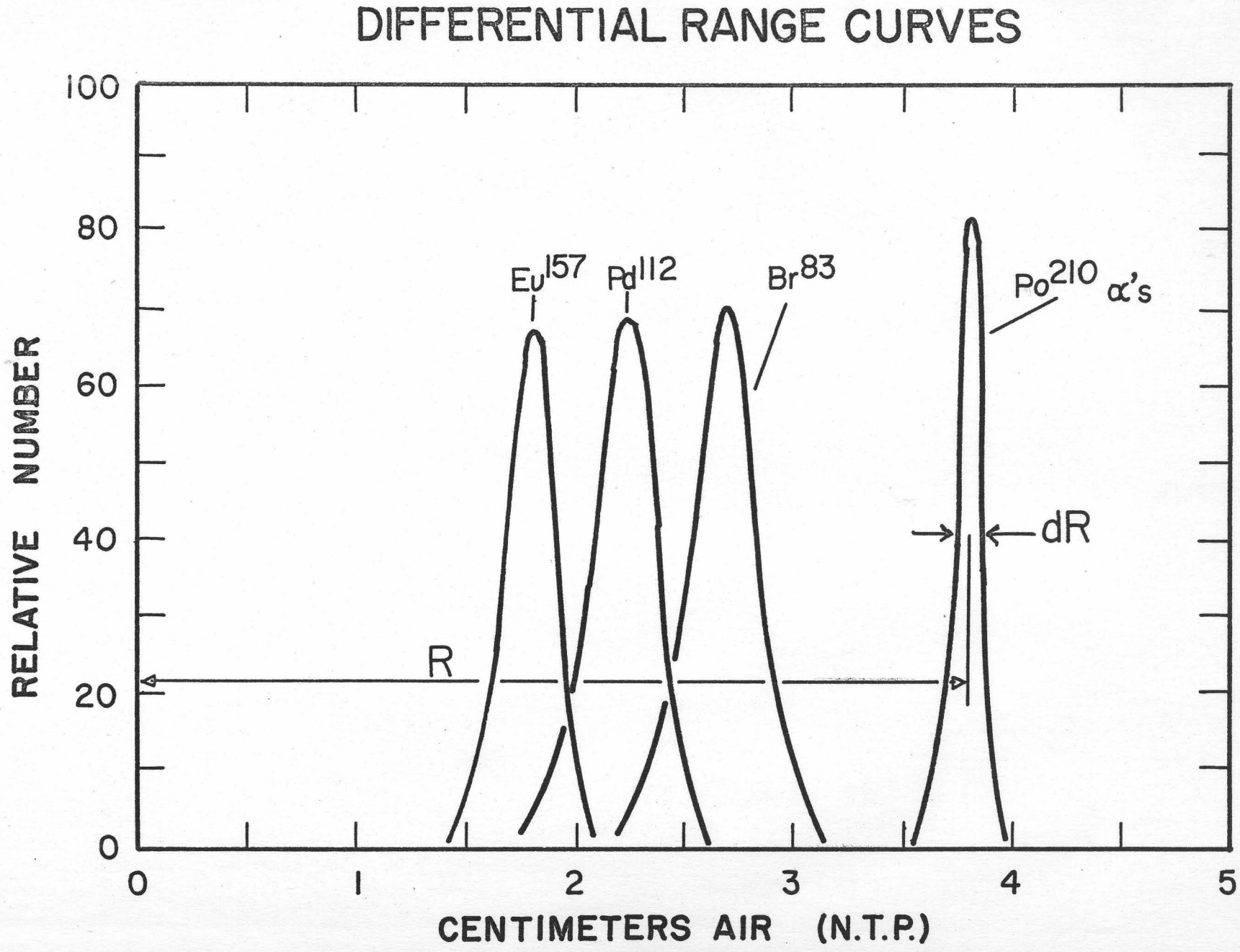
DIFFERENTIAL RANGE CURVES
RELATIVE NUMBER
100
80
60
40
20
0
0
1
2
3
4
5
CENTIMETERS AIR (N.T.P.)
Eu157
Pd112
Br83
Po210 α's
R
dR

FIGURE 4

1.2 b. The Theory of the Slowing Down of Fission Fragments in Matter

Theoretical treatments of the energy loss of fission fragments on passing through matter have been made by several authors (5)(8)(9). These theoretical treatments have been reasonably successful in explaining some of the main features found experimentally. The most complete treatment on the subject has been given by Bohr in 1948 (5).

Bohr's theory results in the following expression for the total energy loss per centimeter.

$$\frac{1}{N}\frac{dE}{dx} = \frac{4\pi e^4}{mv^2}(Z_{1\text{eff}})^2 Z_2 \log \frac{1.123\, mv^3}{\omega e^2 Z_{1\text{eff}}}$$

$$\frac{4\pi e^4}{M_2 v^2} Z_1^2 Z_2^2 \log \left\{ \left(\frac{M_1 M_2}{M_1 + M_2} \right) \left(\frac{v^2 a_{12}^{sct}}{Z_1 Z_2 e^2} \right) \right\} \qquad (1)$$

in which N = number of atoms of stopping medium per cubic cm

M_1 = mass of fragment

M_2 = mass of stopping material atoms

Z_1 , Z_2 = atomic numbers of the fragment and stopping atoms respectively

e,m = electronic charge and mass

$Z_1 eff$ = effective charge on fragment (~20e initially)

a_{12}^{scr} = impact parameter, beyond which the energy loss is effectively zero owing to the screening of the charges of the nuclei by the atomic electrons. a_{12}^{scr} may be estimated roughly from the Thomas-Fermi model of the atom.

v = the velocity of fragment

w = I/h is the average oscillation frequency of the electrons in the stopping atom (I is the average ionization potential of the electrons of the stopping atom).

In the above equation, the first term expresses the energy loss of the fragment due to the electronic excitation and ionization of the stopping atoms. The second term describes the transfer of energy by "nuclear" collisions.

At the beginning of the range, $Z_1 eff$ (the effective net charge on the fragment) is about 20e. Because of this high value, the electronic stopping term in Eq. 1 is dominant. However, towards the end of the range, the fragment has slowed down and in doing so has aquired more electrons. $Z_1 eff$ thus drops to a low value toward the end of the range and the nuclear stopping term becomes the more important.

A theoretical calculation using Eq. 1 requires some knowledge of the quantity $Z_1 eff$. $Z_1 eff$ will change as the fragment passes through matter since the fragment

continuously gains and loses electrons. Thus the problem of calculating $Z_1 eff$ as a function of fragment velocity must be considered. Bohr (1941) (8) made the assumption that a fragment will lose all those electrons whose orbital velocities are less than the fragment velocity.

It is easily shown that Eq. 1 describes the general features of fission fragment straggling. The first term:

$$\frac{4\pi e^4}{mv^2} (Z_1 eff)^2 \; Z_2 \log \frac{1.123\, mv}{\omega e^2 Z_1 eff}$$

handles the electronic stopping. This, being a many interaction process, results in very little straggling. Each individual electronic interaction will deviate the fragment infinitessimally. The second term, however:

$$\frac{4\pi e^4}{M_2 v^2} Z_1^2 Z_2^2 \; \log \left\{ \frac{M_1 M_2}{M_1 + M_2} \cdot \frac{v^2 a_{12}^{scr}}{Z_1 Z_2 e^2} \right\}$$

describes the so-called nuclear interaction and becomes more important toward the end of the range. The nuclear interactions are responsible for some of the straggling observed. Nuclear interactions generally result in much larger energy transfers than ionization interactions. They are also capable of causing large angle scattering of the fragment, thus contributing effectively to the straggling

observed experimentally.

It can be seen that the second term shows a dependance on the masses and atomic numbers of the fragment and stopping atoms. The logarithmic term:

$$\log\left\{\frac{M_1M_2}{M_1+M_2}\ \frac{v^2a_{12}^{scr}}{Z_1Z_2e^2}\right\}$$

is not very sensitive to changes in M_1, M_2, Z_1 or Z_2. However, the coefficient

$$\frac{Z_1^2Z_2^2}{M_2v^2}$$

indicates that the nuclear interactions, and therefore the straggling attributable to this cause, should depend on $Z_1^2Z_2$ (taking $Z_2 \propto M_2$). This implies that one should expect a greater amount of straggling for heavier fission fragments and also a greater straggling as the atomic number (Z_2) of the stopping material is increased.

1.3 Methods of Determining Fission Fragment Ranges

Since the discovery of fission, many workers have been concerned in the determination of fission fragment ranges and stragglings. There are two distinct approaches to the measurement of fission fragment ranges. The first approach, the individual particle method, involves the study of the tracks of individual fragments. The second approach

employs activity distribution methods, in which the distribution of activities, the result of many fissions, is studied.

The techniques of the individual track method include cloud chamber investigations (11)(12), nuclear emulsion observations (13)(14), and electron microscope studies (15)(16). These techniques enable the scattering of fragments to be investigated statistically (17) and also show how the scattering increases as the mass of the stopping material is increased. In most of the individual track experiments, it was possible to discern the heavy and light groups of fragments by the observation of the short and long tracks respectively. The disadvantage to the individual particle method is that it is impossible to identify either the mass or the atomic number of any given fragment.

The activity distribution technique, usually employing stacked foils, has been widely used (18-29). The advantages of this technique are that the ranges and in some cases even the differential distributions in range of specific mass chains can be determined. The activity distribution technique utilizes the activities of the β^- and γ decays of the fission products themselves -- the self indication technique.

1.4 Results to Date

The ranges of many fission product mass chains have been determined in various stopping materials. A

comprehensive list of the results of previous determinations is given in Table I. It can be seen from this table that the precision in range determinations has increased steadily over the past two decades. Only a few of the measurements however, have enabled differential distributions to be obtained. The work of Suzor (1947)(22), using the stacked foil technique, was one of the earliest experiments which enabled range distributions and stragglings of a few mass chains to be obtained. However, the differential ranges obtained by him were distorted by the fact that he used an uncollimated recoil system.

Probably the best differential range distributions obtained to date are those of Katcoff, Miskel and Stanley (7). These workers used a recoil system in which collimated Pu^{239} fission fragments passed through air at 120 or 140 mm Hg pressure. After being brought to rest by the air, the fragments were deposited or stuck on a series of 14 extremely thin Zapon films spaced out along the recoil system. These films were subsequently analyzed radiochemically for specific fission product activities. The measured activities from each film were plotted graphically against the distance of air traversed to yield differential range curves. In this manner, Katcoff et al obtained the differential range distributions of 20 fission product mass chains. Fig. 4 p.(8) shows three typical examples from their work.

TABLE I FISSION FRAGMENT RANGE DETERMINATIONS

Type of Fragments	Fission Reaction	Stopping Material	Method of Range Determination	Range Values	Reference
gross	U(n,f)	air	recoil chamber	~3cm air eq.	Joliot 1939 (30)
gross	U(n,f)	air	cloud chamber	~3cm air N.T.P.	Corson 1939 (31)
gross	U(n,f)	aluminum & paper	stacked foil	~2.3cm air eq.	McMillan 1939 (18)
gross	U(n,f)	air	ion chamber	~1.7cm air NTP	Anderson 1939 (32)
heavy light	U(n,f)	air	differential ion chamber	1.5cm air NTP 2.2cm air NTP	Booth 1939 (33)
gross	U(n,f)	air	cloud chamber	~1cm air N.T.P.	Joliot 1939 (34)
gross	U(n,f)	argon hydrogen	cloud chamber	~2.5cm air eq.	Brostrøm 1940 (11)
heavy light	U(n,f)	argon helium	cloud chamber	1.7 (A) 2.4 (He) 2.5 (A) 3.0 (He)	Bøggild 1940 (12)
Zr-97 Te-132	U(n,f)	aluminum	stacked foil	4.1 3.5 mgm/cm^2 Al	Joliot 1944 (19)
gross	U(n,f)	colloidion aluminium copper silver gold	stacked foil	2.6 mgm/cm^2 3.7 " 5.2 " 6.1 " 11.4 "	Segrè 1946 (20)

TABLE I (CONTINUED)

Type of Fragments	Fission Reaction	Stopping Material	Method of Range Determination	Range Values	Reference
heavy light	U(n,f)	xenon argon helium hydrogen deuterium	Cloud chamber	1.8 2.3 mm 1.9 2.5 air 2.3 3.0 at 1.77 2.11NTP 1.89 2.25	Bøggild 1947 (17)
Kr^{87} Xe^{137} Br^{89} Kr^{91}	U^{235}(n,f)	aluminium	stacked foil	3.98 mgm Al_2 3.21 per cm^2 4.05 3.63	Sugarman 1947 (21)
Zr^{97} Te^{132} Mo^{99}	U(n,f)	aluminium	stacked foil	3.78 mgm Al_2 3.11 per cm^2 3.78	Suzor 1947 (22)
Zr^{97} Te^{132} Zr^{97}	U(n,f)	aluminium " gold	stacked foil	4.16 mgm/cm^2 3.49 10.5	Suzor 1948 (23)
mass nos 83 117 91 127 92 129 93 132 94 133 97 134 99 140 105 143 109 149 112 157	Pu^{239}(n,f)	air	stacked foils in air	2.65 2.08 cm 2.55 2.09 air 2.55 2.09 2.53 2.05 2.52 2.04 2.50 2.04 2.48 1.92 2.42 1.89 2.35 1.82 2.24 1.79	Katcoff 1948 (7)

TABLE I (CONTINUED)

Type of Fragments	Fission reaction	Stopping Material	Method of Range Determination	Range Values	Reference
heavy light	U(n,f)	air	cloud chamber	1.95 cm air N.T.P. 2.54 "	Bøggild 1949 (35)
Ba^{139} Sr^{89}	$U^{235}(n,f)$	air	air recoil technique	1.94 cm air at 2.45 N.T.P.	Freedman 1951 (24)
Ba^{139} Sr^{91}	$U^{235}(n,f)$	air	air recoil technique	1.75 cm air at 2.45 N.T.P.	Finkle 1951 (25)
Ba^{139} Sr^{91}	$Pu^{239}(n,f)$		"	1.85 " " 2.55	
mass no's 89 131 95 140 103 141 129 144	$U^{235}(n,f)$	aluminium	stacked foil	3.74 3.16 mgm 3.64 2.75 Al 3.57 2.69 per 2.34 2.54 sq.cm p,f d,f	Finkle 1951 (26)
Sr^{89} Sr^{91} Ag^{111} Cd^{115} Sn^{123} Ba ^{140}	U^{238} reaction with 335Mev protons and 18Mev deuterons.	Al	stacked foil	4.01 4.26 4.00 4.20 3.44 3.60 3.37 - 3.19 - 3.00 3.10	Douthett 1954 (27)
heavy light	$U^{235}(n,f)$	zirconium	modified stacked foil technique	8.15 microns in 10.1 zirconium	Smith 1959 (37)
20 fission products	$U^{235}(n,f)$	uranium	recoil in uranium metal	data given in figure 5 p. 19	Niday 1961 (29)

The stragglings obtained by Katcoff et al varied between 10.1 and 15.1 percent, but showed no regular variation as a function of mass number. The range straggling was attributed to three causes: the initial kinetic energy dispersion of the fragments, the experimental dispersion caused by the analytical method, and the straggling attributable to the nuclear collision part of the stopping mechanism. The major factor in the observed straggling is due to the first of the three causes.

In Fig. 5a is shown the manner in which the mean range depends on the mass of a fission fragment. Apart from the steadily increasing ranges of the lighter fragments, it can be seen that Katcoff's data (7) indicate a distinct dip in the center region. This suggested that the division of the fissioning nucleus into two equal fragments minimizes the kinetic energy release.

A more recent work by Niday (29) reports the ranges of 20 fission products of U^{235} in uranium metal. Niday's results are also plotted in Fig. 5b for comparison with the work of Katcoff et al. An interesting feature of Niday's work is that the measured ranges of Cs^{136} and Rb^{86} fall about 10% below the expected values for the corresponding mass numbers. Recent work by Brown (38) has shown that the range of Cs^{136} is in fact below what the range for that mass number should be. However, Brown has shown in very clever

Figure 5a shows the range--mass number curve obtained by Katcoff et al (7). The Range is the "extrapolated" range in cm of air at 760 mm Hg and 15° C.

Figure 5b shows the similar results of Niday (29) where the range is the "integral range" expressed in mgm uranium/cm^2. The two points lying well below the line are Rb^{86} and Cs^{136} the "shielded" nuclei.

RANGE - MASS NUMBER CURVES

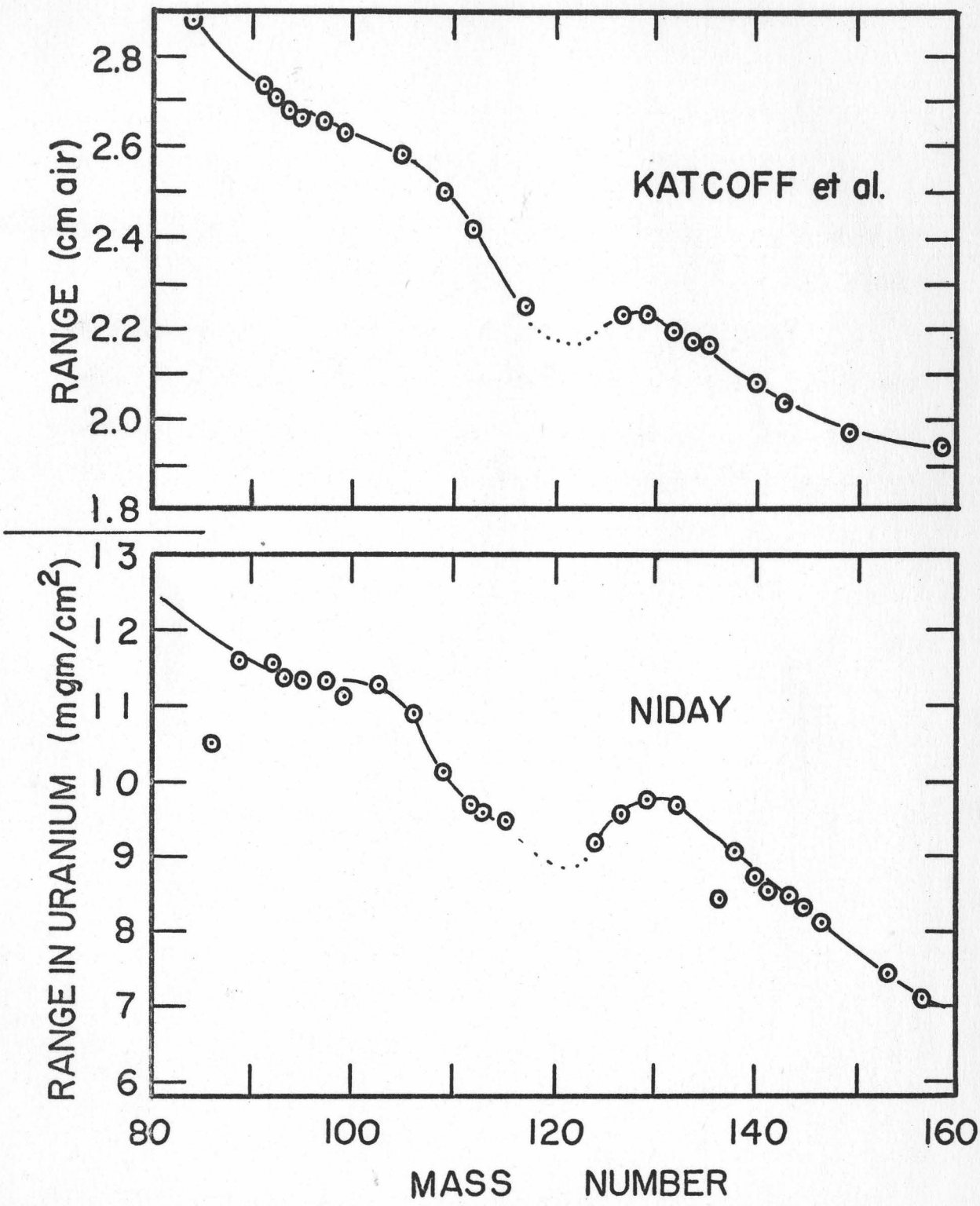

FIGURE 5

arguments that the cases of the shielded nuclei Rb^{86} and Cs^{136} are special cases and using present day knowledge of fission phenomena has accounted for the lower ranges of these nuclides. The technique used by Brown, which shall be described later, was very similar to the one used in this work.

1.5 Aim of this Work

The principal aim of this experimental work is to develop a technique to obtain the most precise range distribution measurements on individual fission fragment mass chains. The differential ranges are to be obtained as free as possible from pertubation effects due to geometry, source thickness, and analytical techniques. The differential range curves are to be obtained in such detail that any shape factors in the distribution can be examined. A test will be made of the prediction of the Bohr theory that the straggling associated with different mass chains should depend on the mass itself.

II EXPERIMENTAL

2.1 General Survey of Experimental Requirements

In this chapter, descriptions are given of the various experimental facets involved in the accurate determination of fission fragment range distributions. It is clear that the following are important features of experimental technique and demand particular attention:

a. The recoil system must be of the well collimated type.

b. The source must be very thin and preferably uniform.

c. The fragment catcher, whether of the stacked foil or other type, must be capable of division into extremely thin layers.

Details are also given of the preparation and counting techniques used, and the γ ray spectroscopic analysis of the fission product activities. The general irradiation arrangement will also be described.

2.2 Design of the Well Collimated Recoil System

The need for a well collimated recoil system is clear, since in any uncollimated system there will be a geometry factor and in order to correct for an appreciable geometry factor, it is necessary to know the nature of the differential range distribution.

The recoil system which was designed for this work is illustrated in Figs. 6 and 7. The source, collimators and catcher are so arranged that no fission fragment emerging from the source can enter the catcher at an angle of greater than five degrees to the normal. A drawing of the recoil system container is shown in Fig. 6 and the sub-assembly of source, collimators and catcher in Fig. 7. The sub-assembly slides into the container, which is equipped with a demountable vacuum seal.

The flight path of a fragment between source and catcher is about 30 centimeters. Thus, a vacuum of better than 0.1 mm Hg is required to ensure that a fragment will lose only a negligible amount of energy before reaching the catcher. The aluminium baffles serve to prevent any fragment from being scattered off the walls of the container into the catcher. When the system is under irradiation, it is connected to a vacuum line via 40 feet of polyethylene tubing. Further details of this may be seen in Fig. 10 of section 2.6 describing the general irradiation set-up.

2.3 Source Preparation

The preparation of very thin and reasonably uniform deposits of fissile material for use as sources of fission fragments is of primary importance. For accurate work, the source must be sufficiently thin that there is no appreciable

Figure 6 shows the construction of the aluminium container used to hold the recoil system. The container is equipped with a dismountable vacuum seal.

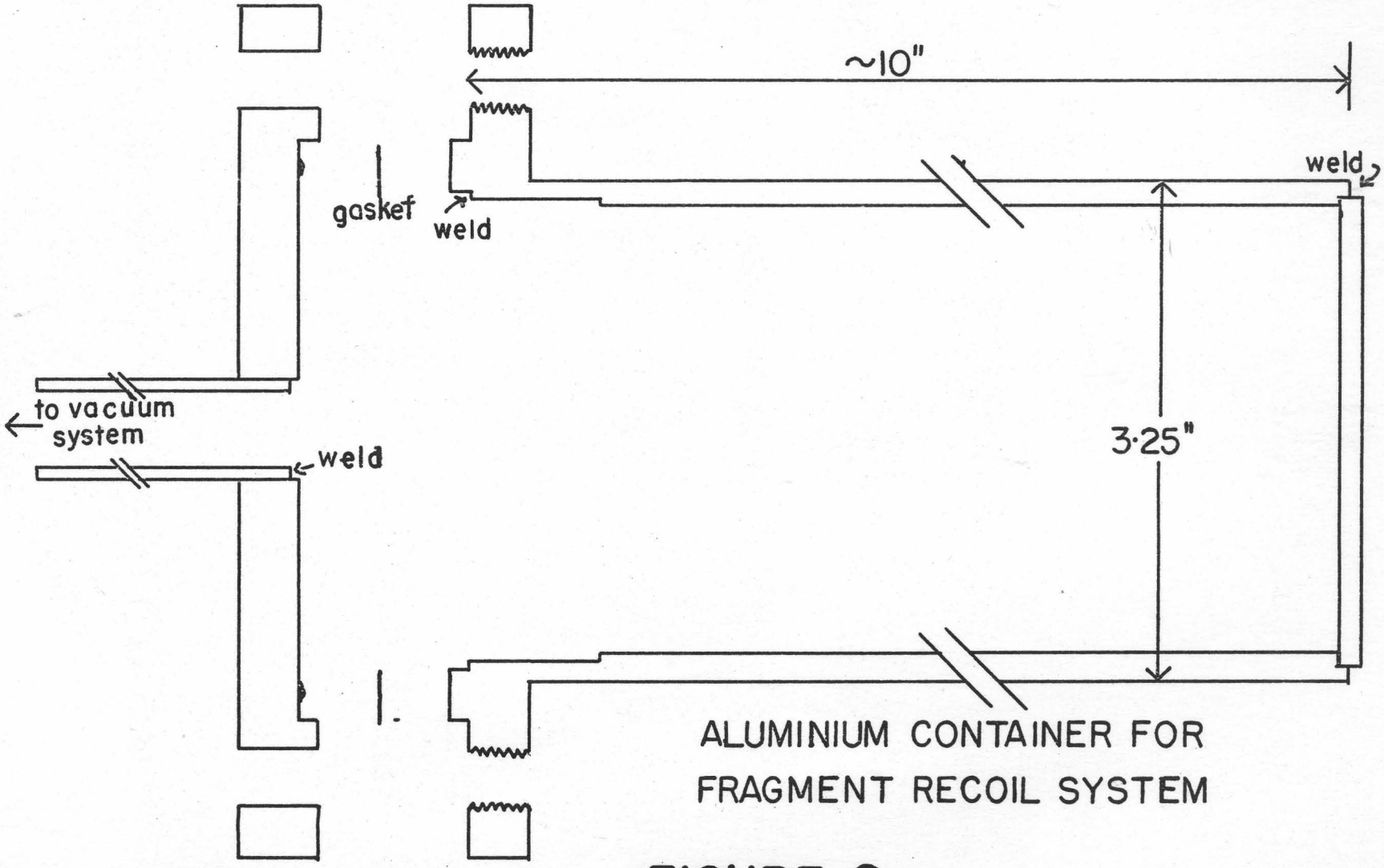
~10"
gasket
weld
weld
to vacuum system
weld
3·25"
ALUMINIUM CONTAINER FOR
FRAGMENT RECOIL SYSTEM

FIGURE 6

Figure 7 shows the construction of the fission fragment collimator. The sub-assembly holds together the source at one end and the catcher at the other end. The catcher is shielded as far as possible with cadmium to prevent neutron activation of impurities in the aluminium catcher.

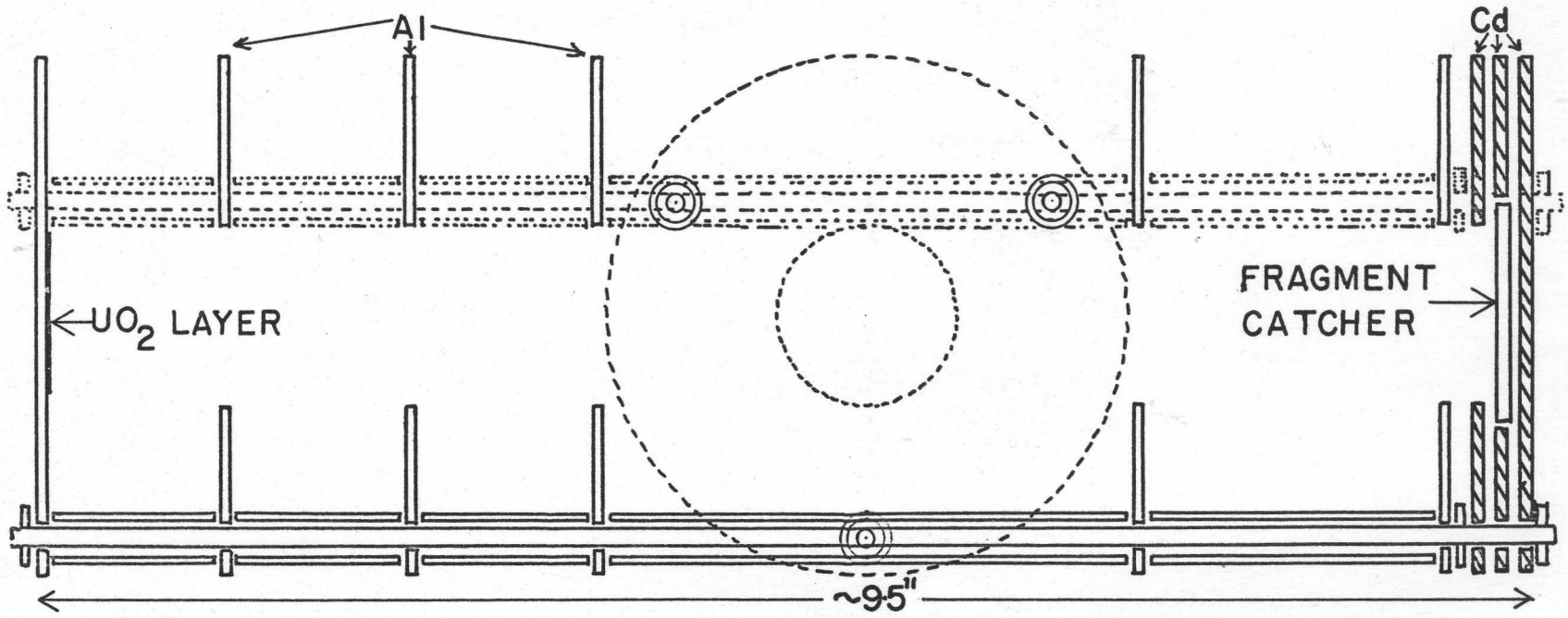

FISSION FRAGMENT COLLIMATOR

FIGURE 7

energy loss of a fragment traversing the source thickness. On the other hand, the source must not be too thin otherwise there will not be enough fissions taking place to give adequate activities in the catcher. The stringent restriction imposed upon the thickness of the fissile layer make the use of enriched fissile material necessary. Calculations indicate that a source thickness of about 10^{-5} cm or less than 100 $\mu gm/cm^2$ will result in about a 1 percent reduction in the range of a typical fission fragment.

Appreciable difficulty is met with in the preparation of such thin deposits of fissile material. There have been various techniques described in the literature and a general reference to the subject has been given by Povelites (39), Geneva Conference 1958. A number of the techniques therein described were tried; only one seemed to yield satisfactory results. A brief summary of the methods employed and their applicability to this work is described below.

a. Painting

In this method a "paint" is made up using cellulose nitrate and acetone according to the method of Glover-Borrel (1955)(40). Uranyl nitrate is then added to the "paint", the viscosity of which must be high and the uranium concentration low. A layer of the paint is applied to the backing material using a fine haired brush. After the paint

is dry it is ignited to about 500° C for ten minutes. The ignition removes the organic matter and leaves behind an adherent deposit of uranium oxides. The painting is repeated many times in order to build up a layer to the required thickness. The uniformity of individual layers is rather poor; however, it improves as more and more layers are applied. The painting technique as above described was tried several times. Sources prepared in this way were used in preliminary experiments, but the results were not very satisfactory. Autoradiographs of the sources showed that the painting method produced quite uneven deposits. It was also felt that repeatedly heating the aluminium backing foil to 500° C may cause some diffusion of fissile material into the aluminium. Because of these difficulties, the painting method was replaced by an electrodeposition technique.

b. Electrodeposition

This involves the electroplating of a uranium compound onto a metallic backing. After ignition of the electrodeposited layer, a hard adherent layer of oxides of uranium is formed. Various procedures have been developed by Seaborg et al (41), Wilson and Langer (42), Brodsky et al (43) and Miskel (44). Most of these electrodeposition techniques appear to work well using a platinum backing but fail to do so with an aluminium backing. The high neutron

fluxes and long irradiation periods employed in this work make platinum unsuitable as a backing material.

The papers by Wilson and Langer (42) and Brodsky et al (43) describe techniques for depositing fissile material onto aluminium. These methods are probably quite good for forming thick layers (i.e. up to 3 mgm/cm^2), but were found to be inadequate for producing the thin coatings of less than 100 μgm/cm^2 required for this work.

c. Vacuum Deposition

The technique of vacuum deposition is a standard one for producing very uniform, controllable-thickness films of many materials. The manual by Holland (45) describes in detail the technique of vacuum deposition of a great variety of substances. Fissile films can also be formed using these standard techniques. One big drawback however is the rather large quantity of fissile material evaporated. The vacuum deposition technique was not tried since it involves relatively expensive equipment which was not readily available.

d. The Capillary Droplet Method

This technique is quite a recent innovation, being first mentioned by Carswell and Milstead (46) in 1956. A considerable time was spent in refining this technique to produce the required fissile layers needed for this work.

Essentially the procedure consists in firing a minute spray of droplets from a fine capillary tube onto

the backing material. The droplets leave the "gun" under the influence of a strong electric field. A description of the apparatus developed follows.

A diagram of the apparatus is shown in Fig. 8. The essential component is a piece of capillary tubing 6 mm o.d. and 0.5 mm i.d. about three inches long. One end is drawn out to a fine tip and a piece of 1 mil stainless steel wire is pushed down the capillary to within about a centimeter of the fine tip. A column of solution of uranyl nitrate dissolved in acetone is drawn into the fine end of the capillary. A potential of eight to ten thousand volts is put between the fine capillary point and the backing material which is situated about two centimeters away from the tip. Under the influence of the electric field, the solution is slowly ejected from the capillary. The droplets are so tiny that they cannot be seen by the unaided eye. In traversing the distance between the capillary and the backing material, each droplet evaporates all the solvent acetone and the fissile material alone impinges upon the backing material. The diagram shown in Fig. 8 is somewhat more complicated than the bare essentials just described. It shows the provisions which were made to rotate the backing material during deposition and also the mask placed over the backing material to precisely limit the area of the deposit. Provision was also made for sucking air through the apparatus to prevent fissile material from contaminating the air.

Figure 8 illustrates the construction of the droplet gun apparatus used to make very thin uniform deposits of fissile material.

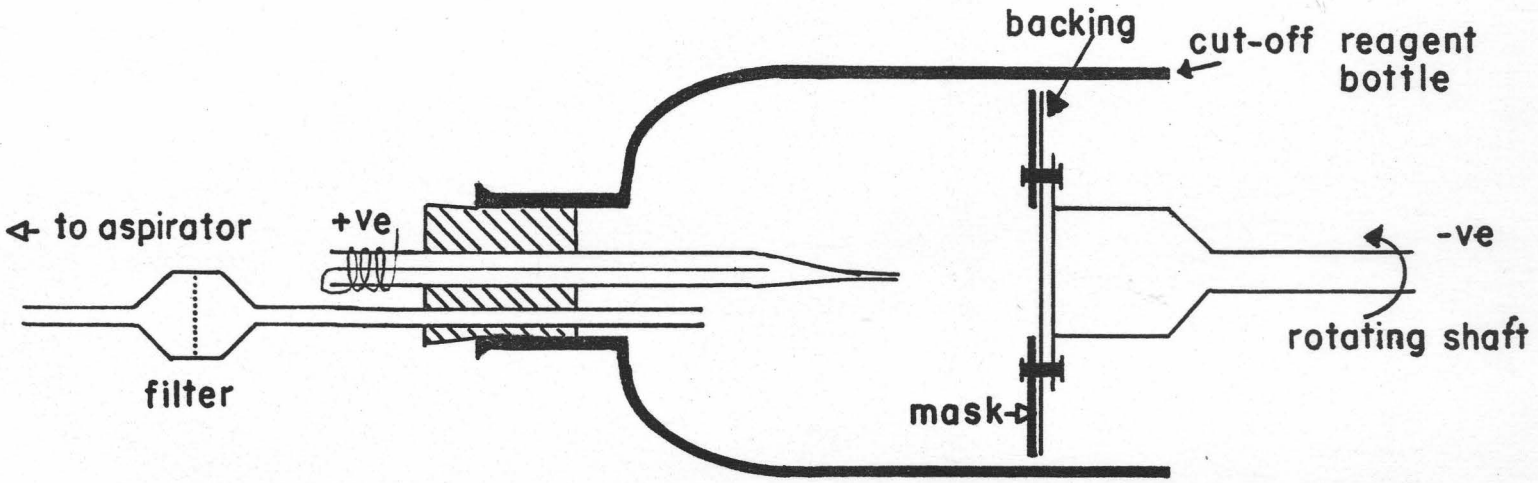

DIAGRAM OF "DROPLET GUN" APPARATUS

FIGURE 8

The deposits formed using this technique were extremely thin and exhibited interference colours depending on the thickness. Autoradiographs of such deposits confirmed that they were very uniform. Before handling, the deposits were ignited to about 500° C for five minutes to produce a very adherent layer of oxides of uranium.

2.4 The Fission Fragment Catcher

a. General considerations

From Table I p.15, it is seen that the ranges of fission fragments in air at N.T.P. lie between 1.8 cm for the heavier and 2.7 cm for the lighter fragments. The corresponding ranges in more dense material such as solids are much shorter. For example according to Niday (1961)(29) the ranges of typical heavy and light fragments in uranium metal are 6.2×10^{-4} cm and 5.6×10^{-4} cm respectively. In aluminium the corresponding ranges would be 1.4×10^{-3} cm and 1.0×10^{-3} cm.

The short range of fission fragments in solid materials makes the accurate measurement of the differential range distributions very difficult. It is clear that in order to make this type of measurement, some technique must be available for the fine division of the stopping material or catcher.

Most commercially available foils are relatively thick in comparison with fission fragment ranges. The use of stacks of commercially available foils can only yield

crude measurements of fission product distributions. In order to overcome this difficulty, two refined techniques were developed in the course of this work which enable the precise range distributions to be obtained. The first technique involved the preparation of extremely thin (20 millionths of a centimeter) films which were uniform and could be used in the stacked foil technique. The second approach, which will be called the anodization-stripping technique, involved anodically forming an oxide layer and then chemically dissolving it. These two methods will now be described in detail.

b. The Use of Thin Films of Aluminium Oxide in the Stacked Foil Technique

It has been known for some time that when aluminium is made the anode of an electrolytic cell using a suitable electrolyte, a layer of aluminium oxide is formed on the surface of the aluminium anode. This is a very interesting phenomenon and is known as anodization. The thickness of the oxide film is linearly dependent on the applied voltage across the cell, Guntherschulze and Betz (1937)(47). In 1951 a technique was developed by Strohmaier (48) to obtain extremely thin films of aluminium oxide by dissolving away the underlying aluminium with hydrochloric acid. In this manner, perfectly uniform films of aluminium oxide can be prepared with the desired thickness. It was realized at the beginning

of this work that films of about 2000 Å such as can be obtained by the anodization process, would be ideal for use in stacked foil experiments. The technical problem of obtaining self supported films, suitable for stacking and mounting in the recoil system was solved as described below.

Circles of three inch diameter were cut from 0.003" commercial aluminium foil. These foils were then lightly spot-welded onto an aluminium frame and immersed in the anodization bath. The bath contained a three percent solution of ammonium citrate as electrolyte. The circular foils were anodized to a voltage of 150 volts, thus producing an oxide layer 2000 Å thick (13.4 Å per volt). After washing and drying the foils, each foil was successively placed in a jig and a three inch diameter mask placed on top. The mask had a one inch diameter concentric hole through which the oxide from one side of the foil could be removed by rubbing with a fine wire brush.

On immersing the foils, suitably mounted in a bath of 6N hydrochloric acid, a vigorous reaction took place which dissolved away the aluminium from the central one inch region. In this manner, films of aluminium oxide 2000 Å thick were manufactured integrally mounted on the surrounding annulus of aluminium foil

Since the range of typical fission fragments in aluminium oxide is expected to be about 0.8×10^{-3} cm,

stacks of about 65 films each 2000 Å thick are necessary to collect all the fragments. Such stacks of the integrally mounted oxide films were made up and used as the "catcher" in the recoil system. After the irradiation period, the foil stack was removed and fission product activities in each film monitored. These results will be discussed later. At this stage, it is necessary to describe the second method developed for the fine division of the catcher into thin sections, namely the anodization-chemical strip technique.

b. Technique of Successive Anodization-Chemical Strip

This technique is an extremely sensitive method for obtaining differential activity distributions and was first developed by Davies et al (1960)(49) at Chalk River. Essentially, the process is as follows.

A catcher foil was made from pure aluminium sheet about 30 mil thick. The catcher was anodized to form an oxide layer and was then immersed in a "stripping solution" which dissolved the oxide off to leave the bare aluminium metal. A repetition of this process resulted in the removal of very thin layers from the aluminium catcher.

The aluminium catcher foil was shaped as in Fig. 9. After irradiation this catcher contained a spatial distribution of all the fission products. First a measured volume of electrolyte (three percent ammonium citrate) was poured into the anodization cell as shown in Fig. 9. The catcher

Figure 9 is a schematic picture of the arrangement used for anodizing the catcher foil in the anodization-chemical strip technique.

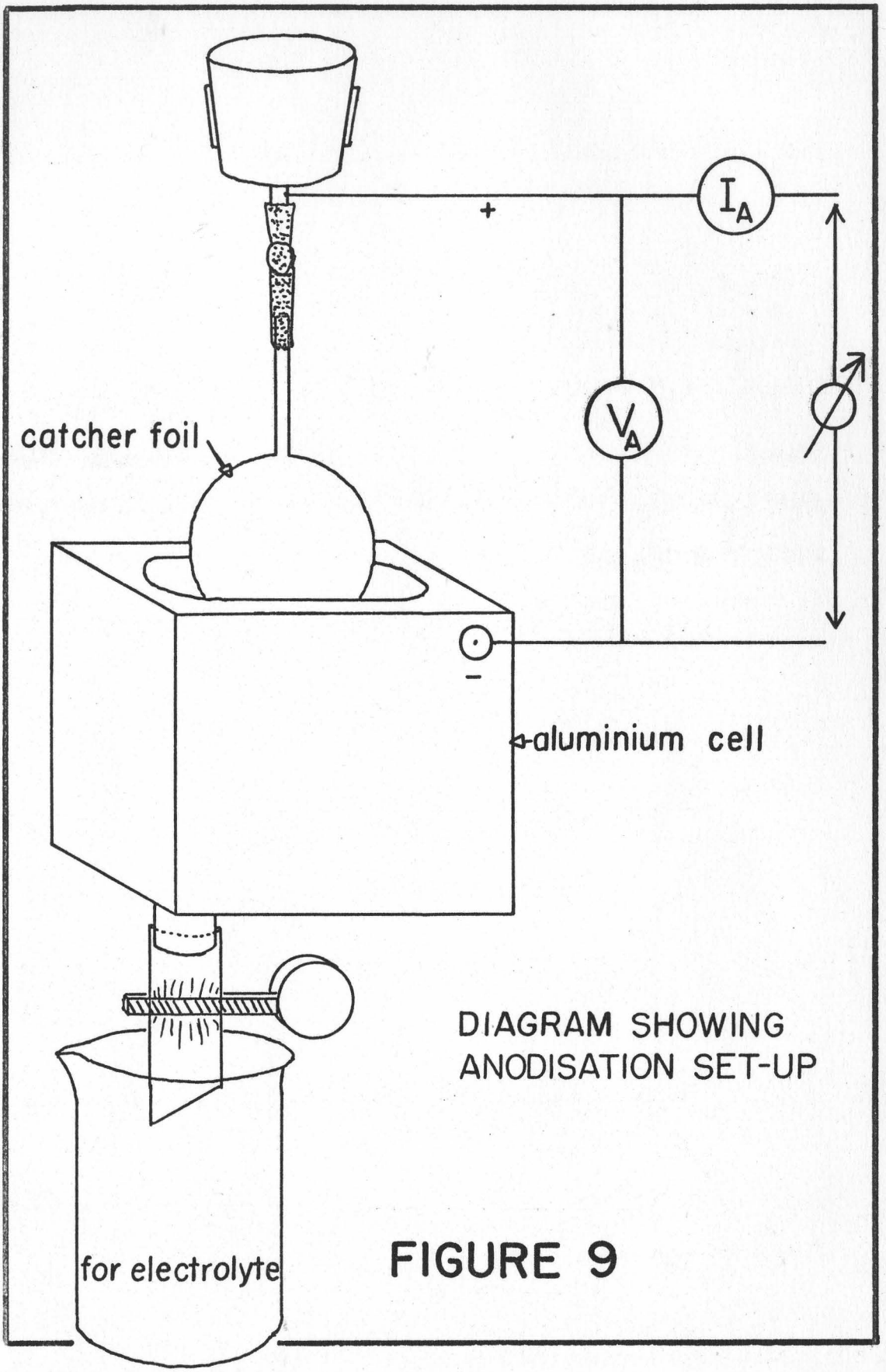

DIAGRAM SHOWING
ANODISATION SET-UP

FIGURE 9

was then immersed in the electrolyte so that the whole of the circular portion was covered by electrolyte, but the connection tag was kept out of the solution. The catcher was then anodized to 150 volts, forming an oxide layer 2000 Å thick on its surface. In doing this, about 1000 Å of superficial aluminium was oxidized. After anodization the catcher was carefully removed from the cell and any adhering electrolyte washed off into the cell. The foil was then ready for "stripping". This was done in a small volume of three percent chromic-phosphoric acid at 95° C. After a three minute immersion in the stripping solution, all the oxide formed during anodization was dissolved off. Since stripping solution does not attack the metal, the reaction ceased when the oxide layer had been removed.

A repetition of the above process was used to remove successive thin layers of aluminium. Each anodization and each stripping solution contained some of the fission product activity originally in the catcher. These solutions were kept for sample preparation as described in section 2.5 a. In all, about 120 anodization-stripping operations were necessary to remove all the fission product activity from the catcher foil.

2.5 Sample Preparation and Counting Procedure

As mentioned in the introductory section, the fission products are β^- and γ active. In principle, both

of these radiation types can be used to monitor the activities present in the samples obtained from the stacked foil and anodization-stripping experiments.

The counting samples from the aluminium oxide thin film experiments were prepared by spraying the film and surrounding aluminium foil with a fast drying varnish. Then while the varnish was still tacky, the film was pressed down over a standard one inch sample container so that the whole of the film adhered to it. When dry, the surrounding aluminium annulus was torn away leaving a nicely mounted sample for counting. These samples could be monitored for both β^- and γ activity.

The samples from the anodization-stripping experiments were left in liquid form. For a convenient counting geometry the volume was reduced by evaporation. These samples were only used in the γ ray analysis of activities.

2.6 General Irradiation Facility

The McMaster Nuclear Reactor is of the swimming pool type. This form of reactor is ideally suited for experiments of this kind in which equipment must be placed near the reactor core. The thermal neutron flux at the centre of the core face is in the range of 10^{12} - 10^{13} neutrons/cm^2/sec when the power level is one megawatt. This flux is quite sufficient for experiments of the kind involved in this

work. A general view of the experimental facility is shown in Fig. 10. An ordinary mechanical pump was used to provide the necessary vacuum in the recoil chamber.

Since activity is not allowed to enter the reactor exhaust system, a cold trap was installed. The cold trap contained activated charcoal and was placed immediately before the pump as shown in Fig. 10.

Figure 10 shows the general arrangement of the apparatus during irradiation.

GENERAL LAYOUT DIAGRAM

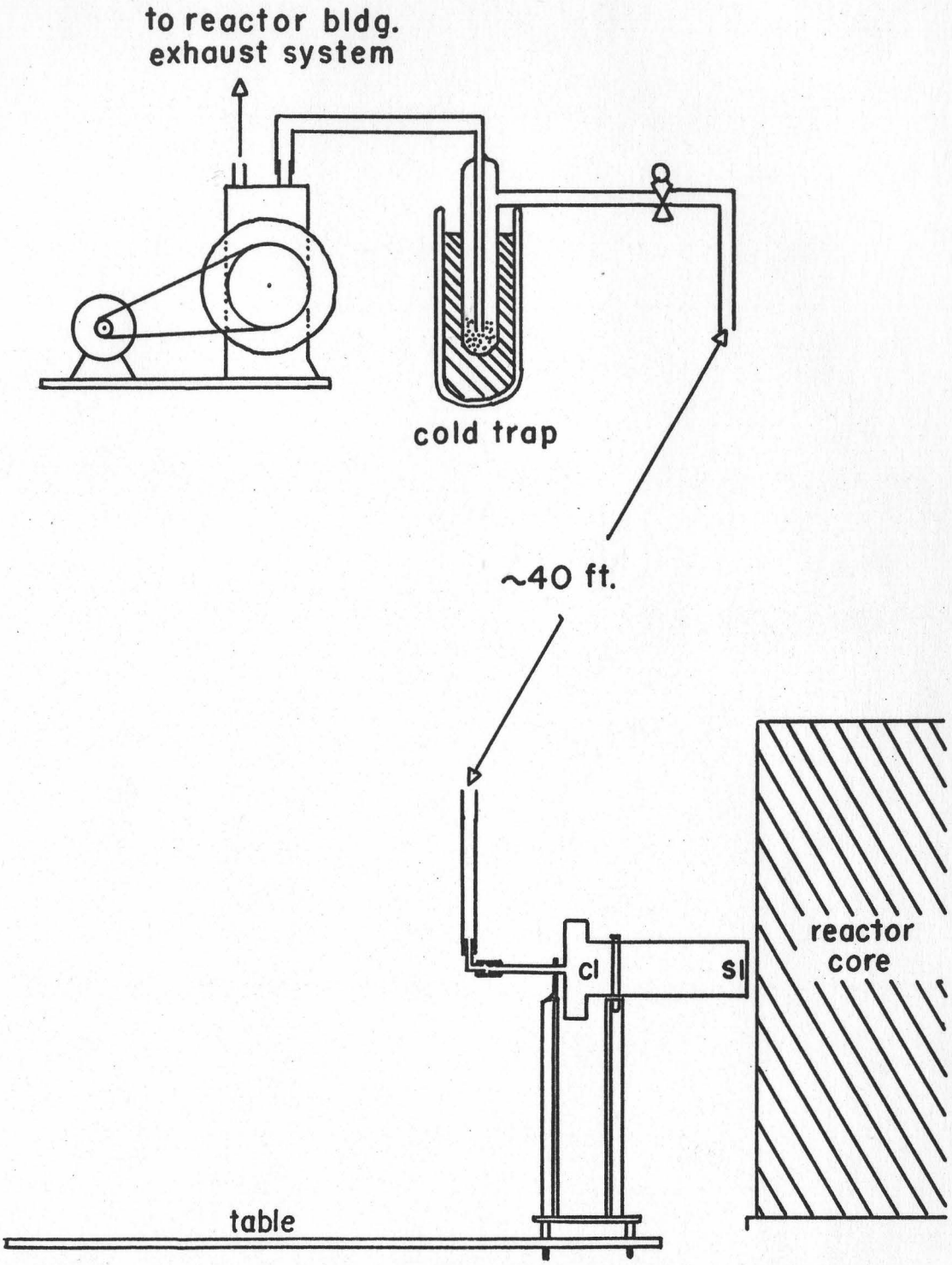

FIGURE 10

III RESULTS

3.1 General

This chapter falls into three subdivisions: Section 3.2 gives the results of early experiments using stacked films of aluminium oxide in the determination of fission fragment ranges.

Section 3.3 describes the results of certain preliminary investigations which were conducted on the anodization-stripping technique. These experiments were performed in order to find out more information on this technique so that the suitability of its use in fission fragment range studies could be assessed.

Section 3.4 gives the results of several range and straggling measurements made using the anodization-stripping technique.

3.2 Early Experiments Using Stacks of Aluminium Oxide Films

One of the principle aims of this work was to obtain accurate measurements of fission fragment ranges and their stragglings. The arguments presented in section 2.4 a. showed that a feasible method of achieving these aims was the use of stacks of very thin films of aluminium oxide. A stack of 60 aluminium oxide films 2000 Å thick was used for the catcher. The assembly which was contained in

polyethylene was irradiated for 24 hrs.

The results of this experiment, which is typical of several are shown in Fig. 11. Here, the gross beta count from each film is shown as a function of the film number in the stack. It can be seen that the results were very unsatisfactory since the light and heavy fragment ranges are not resolved. Possible reasons for the poor results are:

a. In this experiment a "thick" uranium source was used - the preparation of very thin sources as described in section 2.3 d. was not at that time developed.

b. This experiment was done using a recoil system container made of polyethylene. Polyethylene was chosen for its low activation, but, unfortunately it generates large quantities of hydrogen under neutron and γ ray irradiation. The hydrogen generation made it difficult to maintain a good vacuum in the recoil chamber. The presence of an appreciable pressure build-up in the chamber decreased the range of fission fragments in the aluminium oxide films.

c. According to Berman et al (50) aluminium oxide is particularly susceptible to radiation damage caused by fission fragments. This is probably the cause of considerable film breakage which makes sample preparation and counting difficult.

d. Gross beta counting, unaided by chemical separation

Figure 11 shows the distribution of beta activity in the stack of aluminium oxide films.

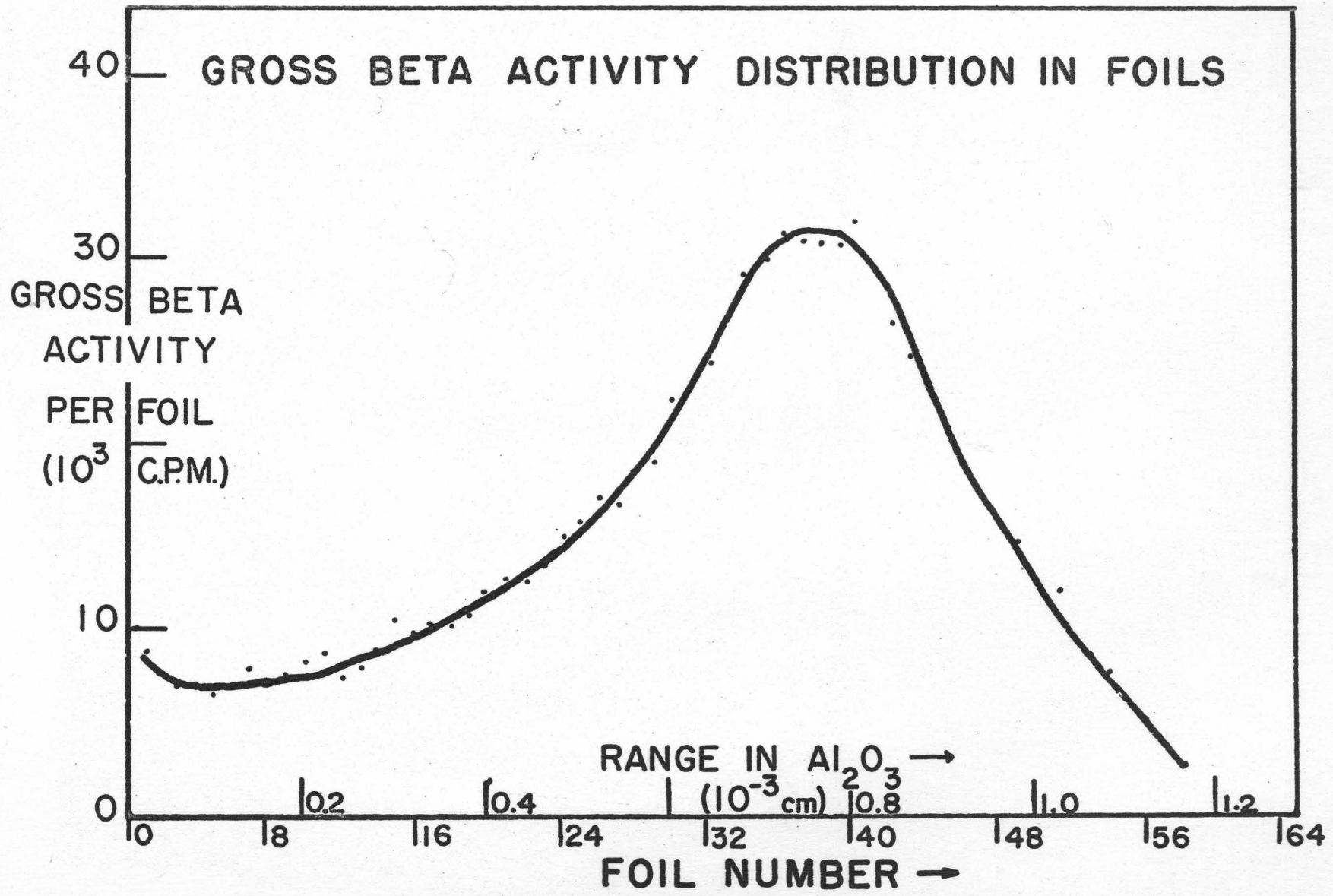
GROSS BETA ACTIVITY DISTRIBUTION IN FOILS
40
30
10
0
GROSS BETA ACTIVITY PER FOIL (10³ C.P.M.)
RANGE IN Al2O3 → (10⁻³ cm)
0.2
0.4
0.8
1.0
1.2
0
8
16
24
32
40
48
56
64
FOIL NUMBER →

FIGURE II

is incapable of giving any detailed information on the ranges and stragglings of particular species of fission products. The film activities obtained in this experiment were not sufficient to yield statistically meaningful results using gamma-ray spectroscopy.

In conclusion of this section, it may be said that the stacked film experiments were not too useful. About the only significant information obtained was the maximum gross range of fission products in aluminium oxide i.e. about 1.2×10^{-3} cm. As an afterthought however it may be said that, providing thin fissile sources are used and providing chemical separation of fission products are used, the method could almost certainly yield satisfactory results.

3.3 Results of Preliminary Experiments on the Nature of the Anodization-Stripping Technique

When it became apparent that the stacked film technique, as described above and in section 2.4 b., presented several severe difficulties, it was decided to try other possible techniques. It came to notice that a group of researchers at Chalk River, namely Davies et al (49), had recently developed a technique for the determination of the ranges of heavy ions in the kev region. Furthermore, this technique had been applied to the problem of determining the ranges of Cs^{136}, Cs^{137} and Ba^{140} fission

fragments in aluminium, Brown and Oliver (1960)(38). A program was therefore undertaken to make use of this technique in this work.

Owing to a lack of information on the details of the anodization-stripping technique, it was decided to conduct preliminary experiments to test the suitability of the technique for achieving the aims of this work.

The following tests were performed; a. the relative rate of attack of the stripping solution on the oxide and on the metal was investigated. b. Experiments were undertaken to determine how the rate of dissolution of the oxide in the stripping solution depended on the temperature. c. Tests were made to investigate the uniformity of the layers obtained with this process.

a. Experiments to examine the relative rate of attack of the stripping solution on the oxide and on the metal were conducted. To do this, a piece of aluminium foil 3 cm square was anodized to 150 volts, washed, dried and weighed. The foil was then immersed for successive periods of time in a bath of stripping solution maintained at 95° C. After each period of time the foil was removed, washed, dried and weighed. In this way the amount of oxide removed could be obtained as a function of the time in the stripping solution. The results are given in Table II and are also presented graphically in Fig. 12. It can be seen that a 150 volt anodic oxide layer is completely removed within about

TABLE II

Results of experiment to measure the rate of attack of the stripping solution on the oxide and on the metal

Time in the stripping solution (min)	Weight of the foil and oxide (milligrams)* ± 0.02
0.0	337.99
0.5	337.80
1.0	337.60
1.5	337.40
2.0	337.21
2.5	337.01
3.0	336.87
3.5	336.84
4.5	336.84
6.5	336.82

* measured to the nearest 0.01 mgm

These results are shown graphically in Fig. 12

Figure 12 is a graph illustrating the rate of removal of oxide layer when immersed in the stripping solution held at constant temperature. It can be seen that after about three minutes, effectively all of a 2000 Å oxide layer has been removed.

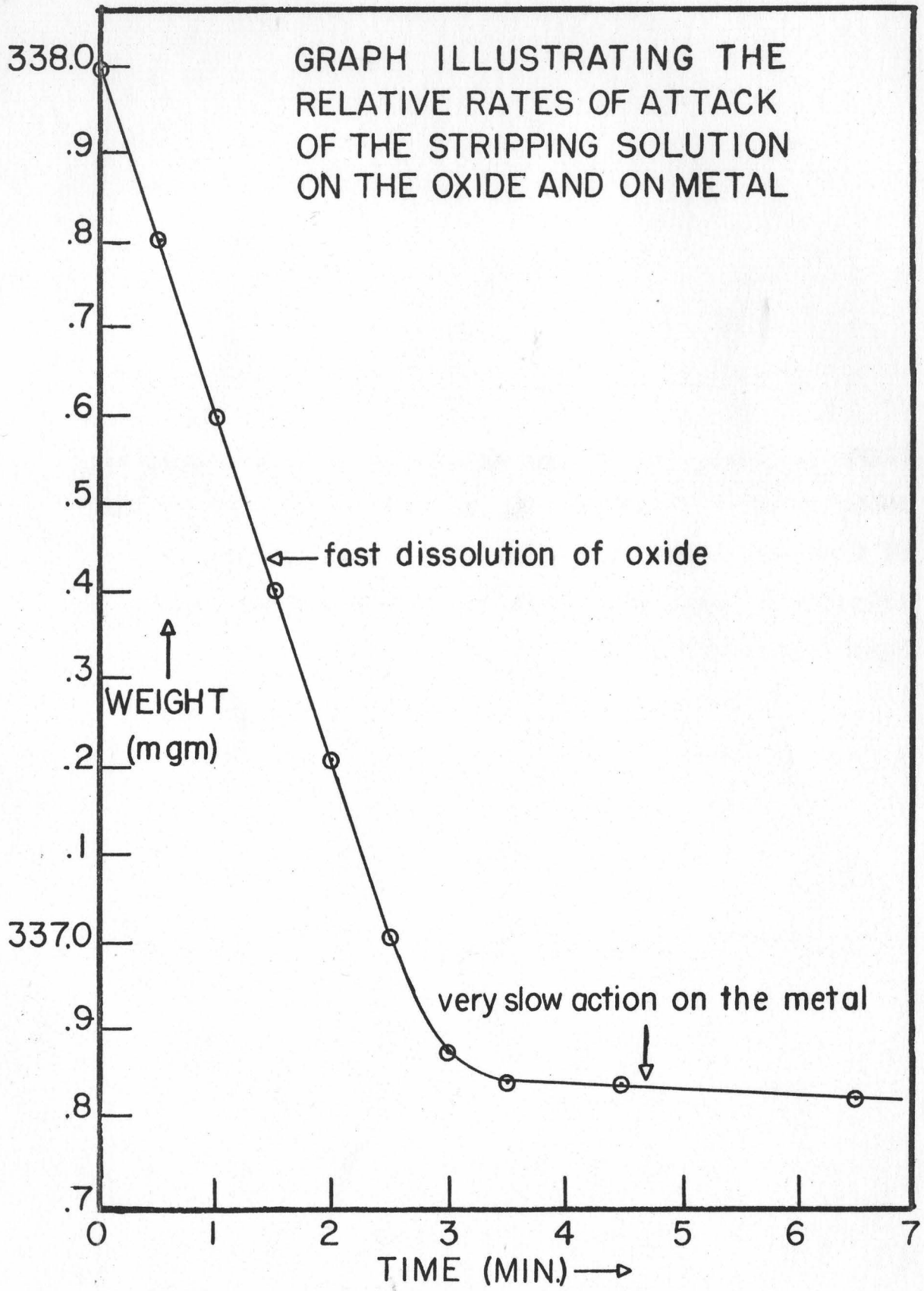
GRAPH ILLUSTRATING THE
RELATIVE RATES OF ATTACK
OF THE STRIPPING SOLUTION
ON THE OXIDE AND ON METAL
338.0
.9
.8
.7
.6
.5
.4
.3
.2
.1
337.0
.9
.8
.7
WEIGHT
(mgm)
fast dissolution of oxide
very slow action on the metal
0
1
2
3
4
5
6
7
TIME (MIN.)

FIGURE 12

three minutes immersion in the stripping solution. From the slope of the graph shown in Fig. 12, it can be seen that the relative rate of attack on the oxide is much greater than on the metal.

b. Results of determination of the temperature dependance of the dissolution power of the stripping solution.

It was necessary to know the effect of the temperature on the dissolving power of the stripping solution because its temperature in the later experiments was not to be accurately controlled. This experiment was performed as follows: A piece of aluminium foil was cut to make a square 3 cm by 3 cm with a narrow tag on it to make electrical connection. The square part of the foil was anodized to 150 volts. It was washed, dried and weighed and then placed in a beaker of fresh stripping solution maintained at a definite constant temperature. The foil was immersed for two minutes being continuously agitated. After exactly two minutes the foil was quickly transferred to a beaker of cold water to halt the dissolution at that point. The foil was then dried and reweighed. The loss in weight was recorded. After a further dip in the stripping solution (to remove any remaining oxide) the foil was again anodized to 150 volts and the whole procedure repeated for a different bath temperature. In this way the rate of attack of the stripping solution on the oxide was determined as a function of the temperature. The

results are given in Table III and plotted on semilog scale in Fig. 13. The results show that the rate of removal of oxide is an exponential function of the reciprocal of the absolute temperature of the stripping solution. Calculations show that a three minute immersion in stripping solution at 95° C will remove essentially all of a 2000 Å oxide layer. From Fig. 10 it is also clear that a four minute immersion in stripping solution at any temperature above 90°C will remove all of a 2000 Å thick oxide layer. Therefore the stripping solution was always maintained at a temperature greater than 90° C.

c. The final experiment to be described in this section is the "linearity test", that is to say, a test which examines whether the anodization-stripping process can be repeated many times without distortion effects occurring.

This test was made by periodically weighing a catcher foil during many repetitions of the anodization-stripping cycle. Thus if the weight decreases linearly, then uniform layers are being removed. Fig. 14 shows the weight of a catcher foil as a function of the total cumulative anodization voltage. The errors on individual points of the graph are about the size of the dots within the circles. The graph clearly shows that the technique is in fact extremely linear.

The results of sections 3.3 a., b., and c. showed that the anodization-stripping technique is very well

TABLE III

Results of experiments on the temperature dependance of the dissolving power of the stripping solution.

Temperature (±1)	$\frac{1}{°K} \times 10^3$ (±1)	Weight of oxide removed in 2 mins at °K $\mu gm/cm^2/min$
324	309	1.4
335	300	3.3
344	291	5.0
348	288	7.2
354	283	11.4
358	280	14.2
363	276	20.8
373	268	21.7

(±1.0 μgm)

Figure 13 shows the results of an experiment to determine the temperature variance of the dissolving power of the stripping solution. The solution rate is plotted on a logarithmic scale against the inverse of the absolute temperature of the stripping solution.

FIGURE 13

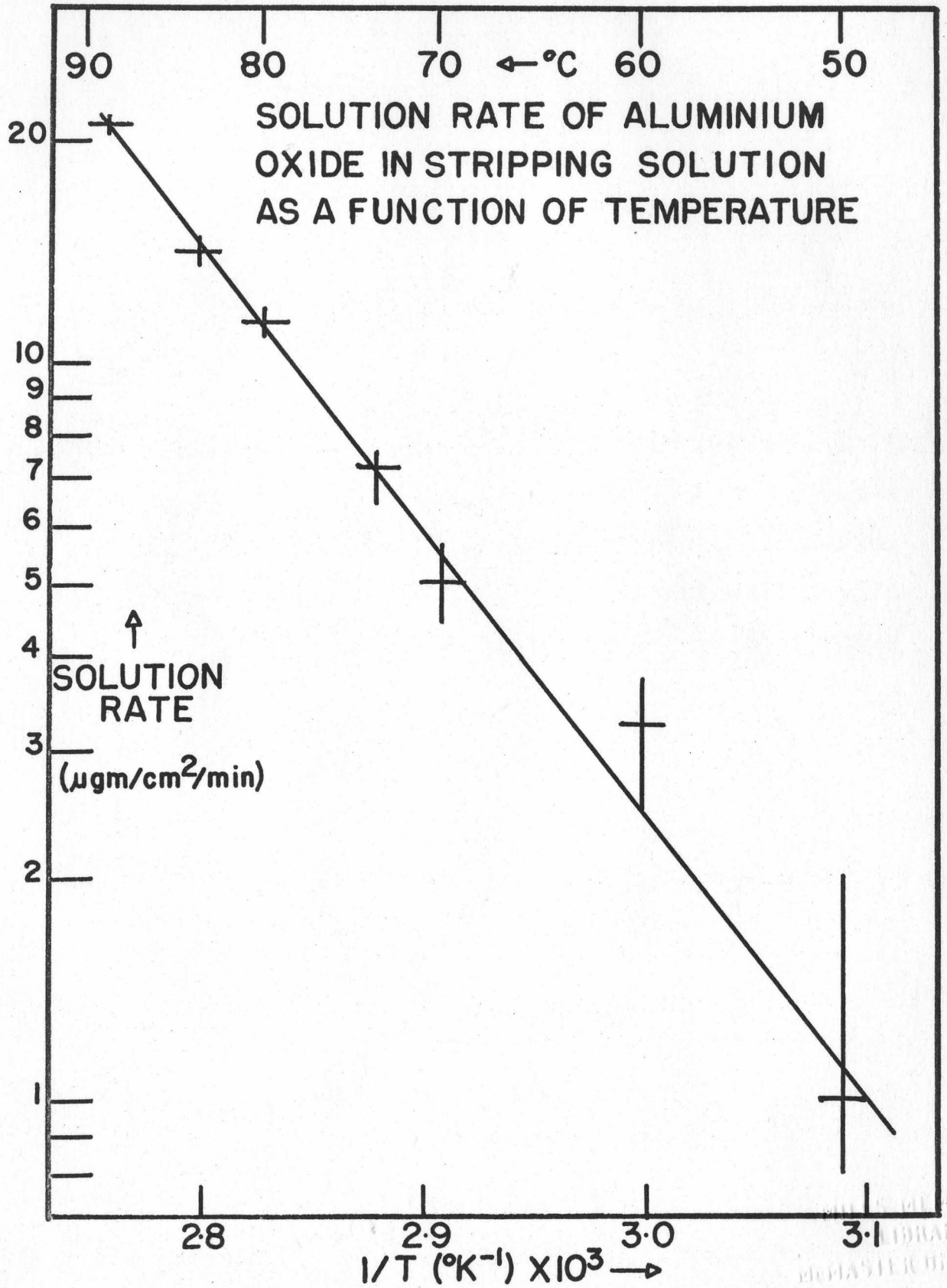
90
80
70 ←°C
60
50
SOLUTION RATE OF ALUMINIUM OXIDE IN STRIPPING SOLUTION AS A FUNCTION OF TEMPERATURE
20
10
9
8
7
6
5
4
3
2
1
SOLUTION RATE
(μgm/cm²/min)
2·8
2·9
3·0
3·1
1/T (°K⁻¹) X10³ →

Figure 14 illustrates the linear removal of aluminium from the catcher foils. About 120 consecutive anodization-chemical strip cycles are represented.

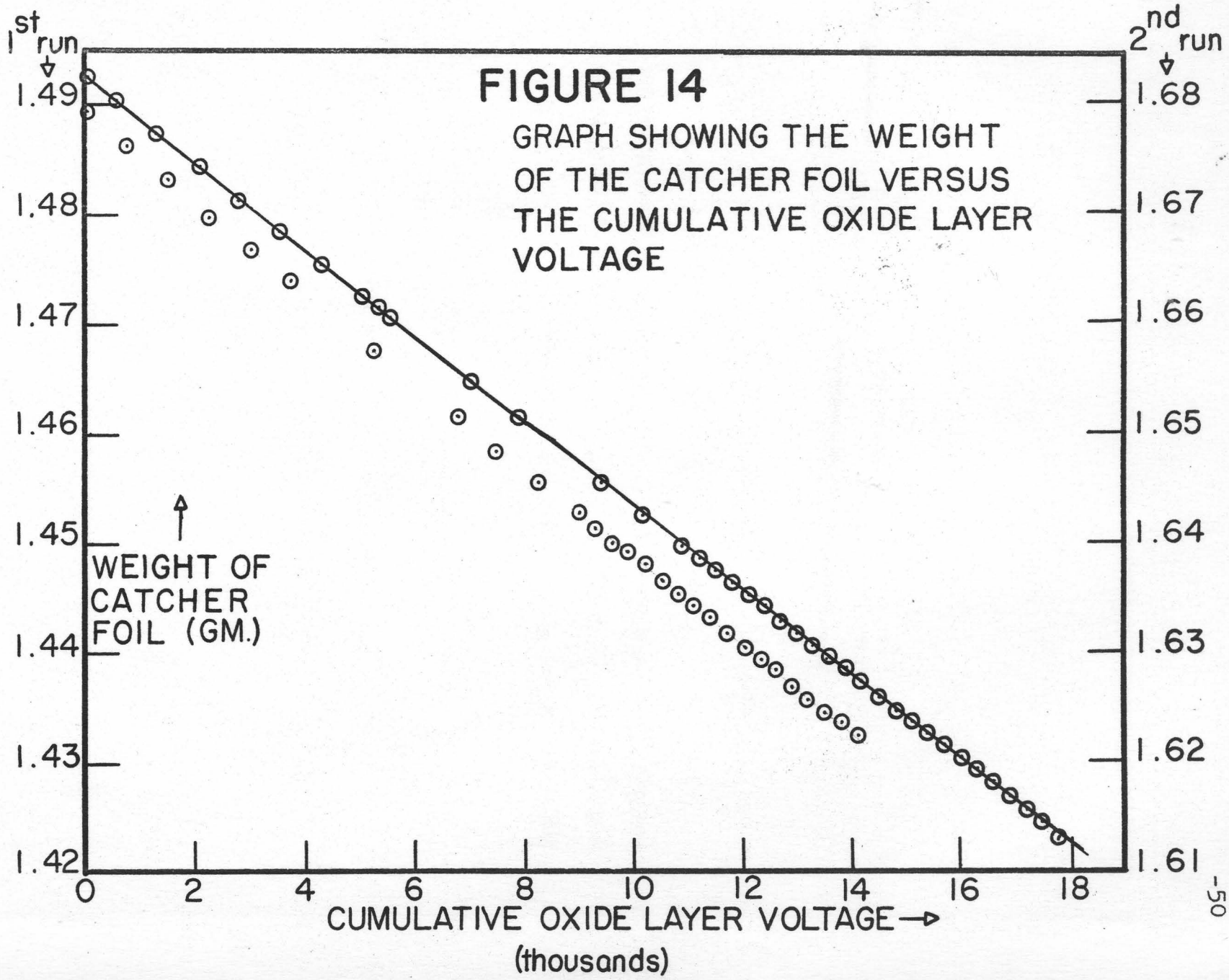

FIGURE 14

GRAPH SHOWING THE WEIGHT OF THE CATCHER FOIL VERSUS THE CUMULATIVE OXIDE LAYER VOLTAGE

understood and that the technique is very reliable for the removal of thin, uniform layers from an aluminium catcher foil. It is therefore an ideal technique for the investigation of fission product ranges and their differential range distributions.

3.4 Range and Straggling Measurements Using the Anodization-Stripping Technique

An examination was made of the decay chains of the fission products formed in the thermal neutron fission of U^{235}. Bearing in mind the restriction imposed by the conditions of this experiment; i.e. that half lives should lie between 10 and 100 days, that yields should be greater than 2 percent and that there should be suitable γ ray emission in decay, one finds that the most suitable nuclides are Nd^{147}, Ce^{141}, Ba^{140}- La^{140} and Zr^{95}- Nb^{95}. Fig. 15 shows the relevant decay chains. Each of these nuclides has one or more prominent γ rays by means of which the activities may be monitored.

The range distributions obtained for the mass numbers 95, 140, 141, and 147 will now be discussed individually.

a. Zr^{95}- Nb^{95}

The decay of Zr^{95} to Nb^{95} proceeds with a half life of 65 days. About 43 percent of the decays produce a γ ray of 760 Kev and 55 percent produce a γ ray of 720 Kev. The

Figure 15 shows the decay chains of fission products of mass numbers 95, 140, 141 and 147. The yields and half lives are also included.

MASS NO. U^{235} FISSION PRODUCT DECAY CHAINS FOR MASS NUMBERS A = 95, 140, 141, AND 147

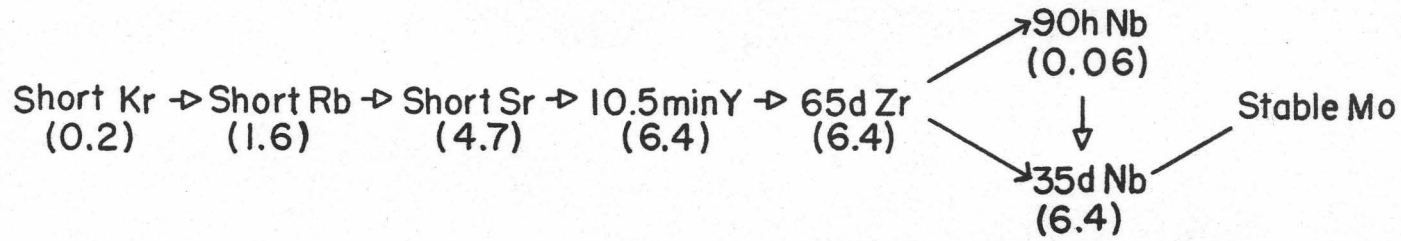

FIGURE 15

subsequent decay of Nb^{95} with a half life of 35 days results in the production of one 762 Kev γ ray for every disintegration. The γ rays of 760-, 726-, and 762 - Kev are of course not resolvable by scintillation spectroscopy and therefore appear as a single broadened line in the region 720-760 Kev.

The determination of the differential range distribution of fragments of mass number 95 therefore consisted in measuring the intensity of the 720-760 Kev triplet for the various samples. The number of counts in the peak at region 720-760 Kev was counted and corrected for background effects. The results are shown graphically in Fig. 16. No correction was made for decay during counting since the half life concerned is very long compared with the total counting period involved.

It is evident from Fig. 16 that the mean range of fission fragments of mass number 95 is 3.78 mgm/cm^2 in aluminium. The straggling is 11.6 percent (full width at half maximum). The distribution is also somewhat screw - this was the only non-symmetrical distribution obtained.

Ba^{140} - La^{140}

From Fig. 15, it can be seen that the fission nuclides formed of mass number 140 decay through 12 day Ba^{140} with its 40 hr La^{140} daughter in equilibrium. The

Figure 16 shows the distribution in range of mass number 95 fission fragments. This was obtained by monitoring the γ ray activity from the Zr^{95}- Nb^{95} decay.

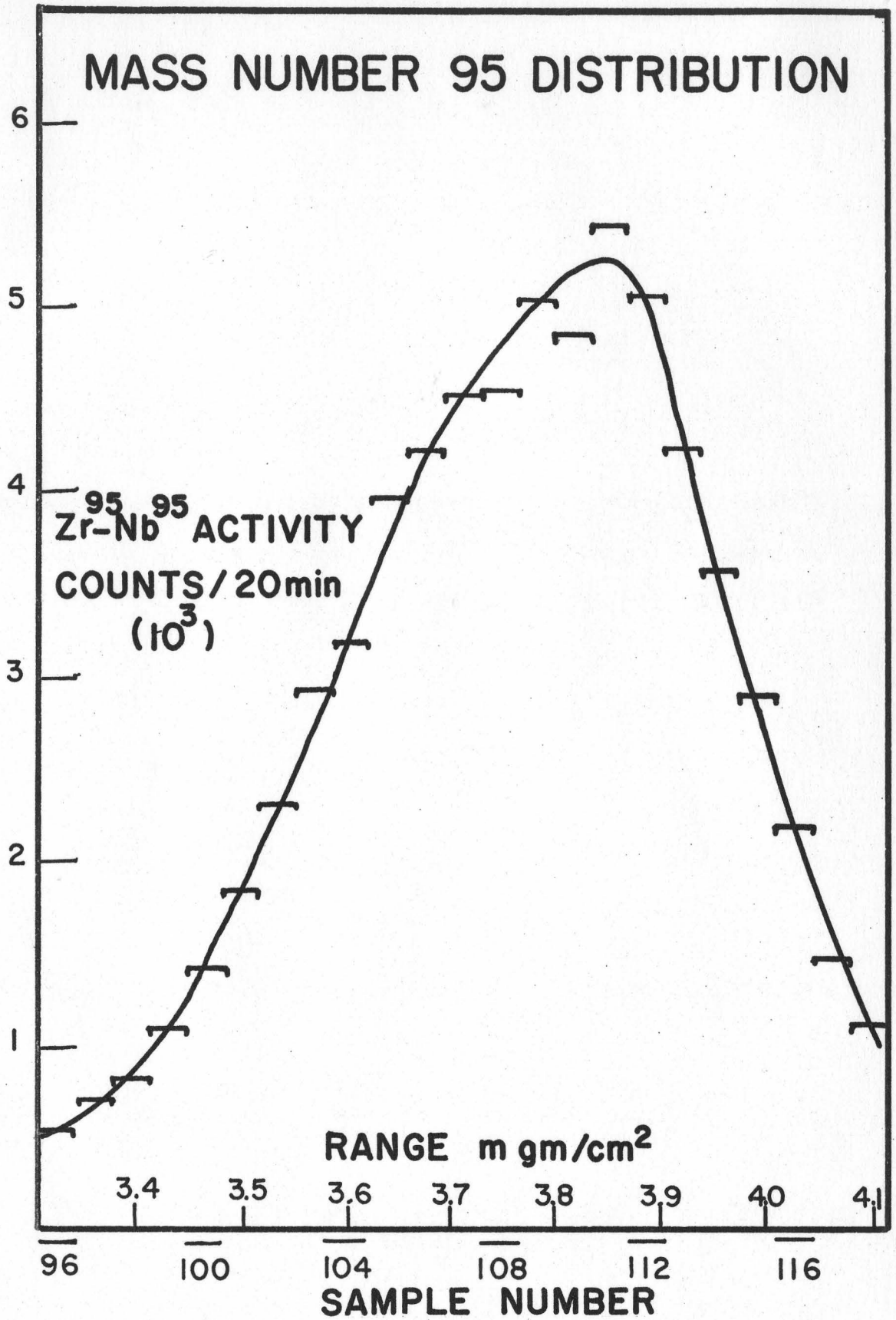
MASS NUMBER 95 DISTRIBUTION
6
5
4
3
2
1
Zr^{95}-Nb^{95} ACTIVITY
COUNTS/20min
(10^3)
RANGE m gm/cm^2
3.4
3.5
3.6
3.7
3.8
3.9
4.0
4.1
96
100
104
108
112
116
SAMPLE NUMBER

FIGURE 16

1.6 Mev γ ray from La^{140} is quite well isolated in the ray spectrum of fission products and therefore provides a convenient activity to measure.

Figure 17 shows the differential range distribution for mass number 140 fragments. This is quite symmetrical, the mean range being 2.94 mgm/cm^2 in aluminium. The straggling was measured to be 14.6 percent.

Ce^{141}

The 32-day Ce^{141} activity is associated with a strong γ ray at 142 Kev. When the samples are counted after some 50-60 days of decay, the 12 day Ba^{140}- La^{140} and the 11.7 day Nd^{147} activities are relatively weak enabling the Ce^{141} activity to be easily measured. As before, the ray spectra of the samples were taken. Using the 142-Kev ray intensity as a Ce^{141} monitor, the distribution for the 141 mass chain was obtained.

The results of the differential range distribution for Ce^{141} are shown in Fig. 18. It is clear from a comparison of Figs. 17 and 18 that there is quite a significant difference in mean ranges of the fragments of mass numbers 140 and 141. This can perhaps be seen more clearly from Fig. 20 in which the various distributions are compared. The mean range of mass number 141 fragments is 2.88 mgm/cm^2 in aluminium and the straggling is 13.9 percent.

Figure 17 shows the distribution in range of mass number 140 fission fragments. This was obtained by monitoring the γ ray activity from the La^{140} decay.

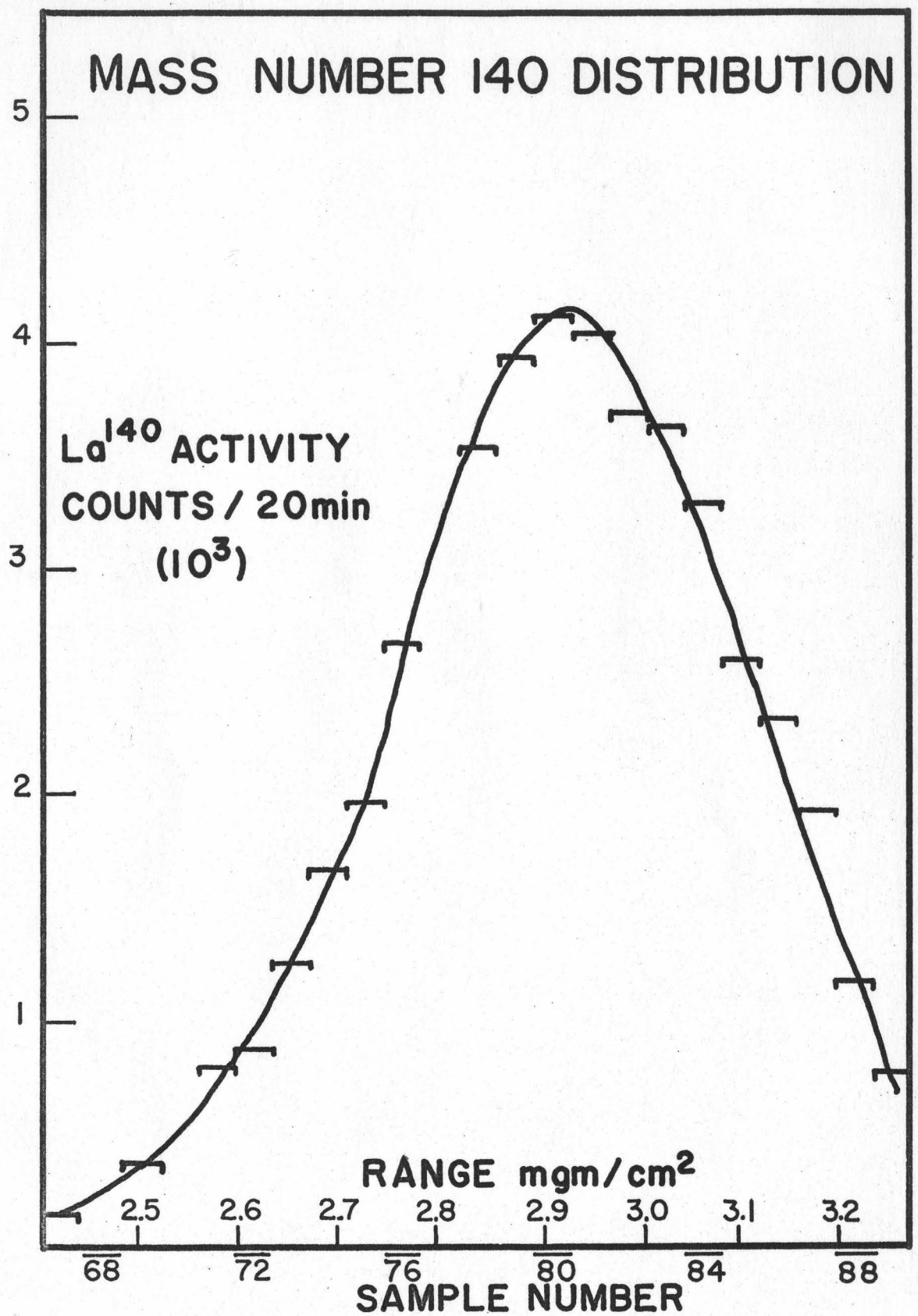
MASS NUMBER 140 DISTRIBUTION
5
4
3
2
1
La140 ACTIVITY
COUNTS / 20min
(10³)
RANGE mgm/cm²
2.5
2.6
2.7
2.8
2.9
3.0
3.1
3.2
68
72
76
80
84
88
SAMPLE NUMBER

FIGURE 17

Figure 18 shows the distribution in range of mass number 141 fission fragments. This was obtained by monitoring the γ ray activity from the Ce^{141} decay.

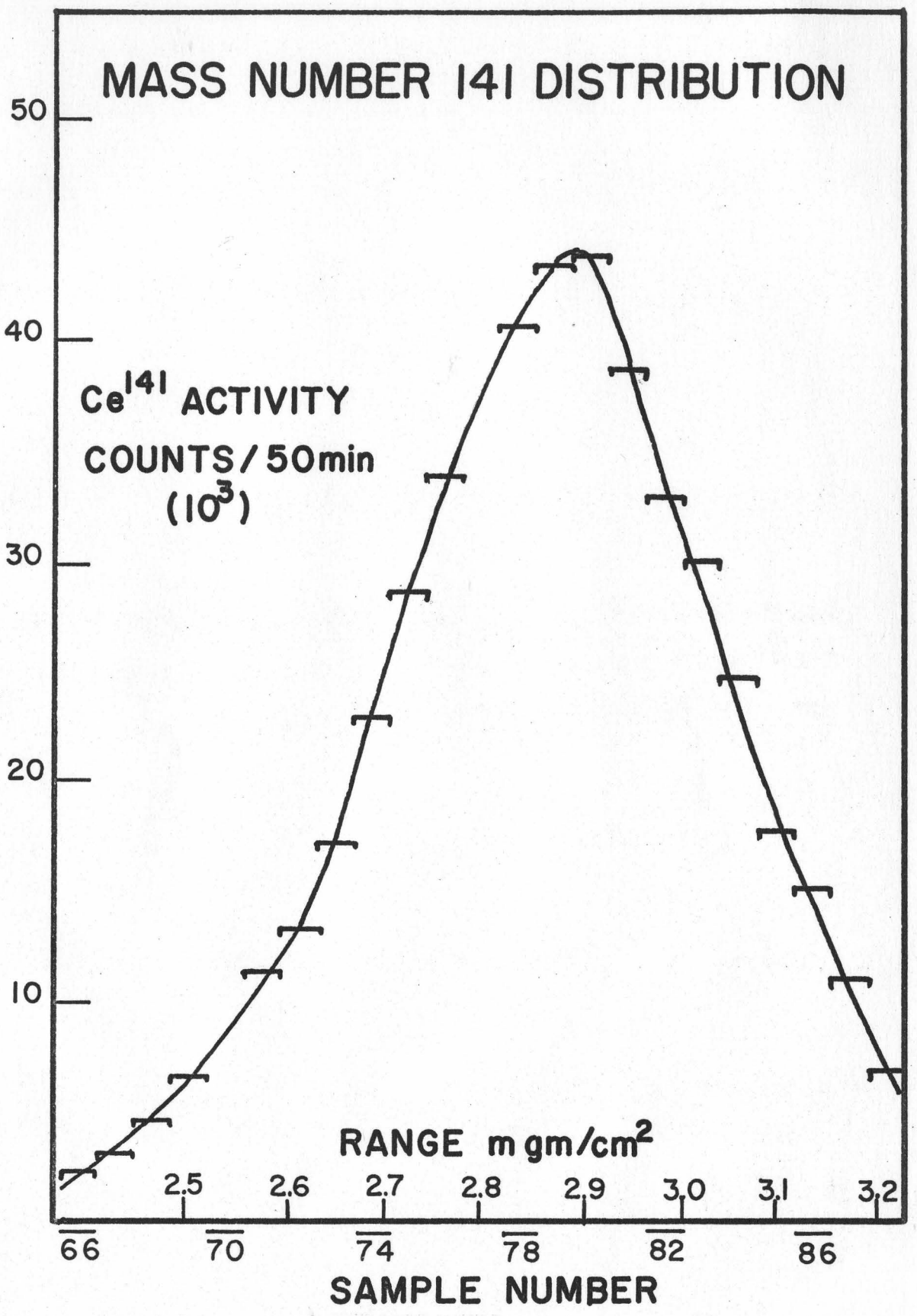
MASS NUMBER 141 DISTRIBUTION
50
40
30
20
10
Ce141 ACTIVITY
COUNTS / 50min
(10³)
RANGE m gm/cm²
2.5
2.6
2.7
2.8
2.9
3.0
3.1
3.2
66
70
74
78
82
86
SAMPLE NUMBER

FIGURE 18

Nd^{147}

As seen from Fig. 15, Nd^{147} has a half life of 11.7 days and decays into a very long lived daughter. The decay of Nd^{147} produces several γ rays, the strongest having an energy of 92 Kev. Unfortunately, the γ ray line at 92 Kev is somewhat disturbed by the activities from Ce^{141}. However, by making up pure samples of Nd^{147} and Ce^{141} and measuring their γ spectra individually, it was found possible to remove the Ce^{141} component from under the 92 Kev Nd^{147} line. The 92 Kev activity of Nd^{147} was therefore used to monitor the range distribution of mass number 147 fragments.

Fig. 19 shows the differential range distribution of Nd^{147} (mass number 147 fragments). The statistics on this graph are not too good because of errors introduced in the γ ray spectra subtraction process which had to be done by hand. It is clear nevertheless that Nd^{147} has a symmetrical range distribution, the mean range being 2.68 mgm/cm^2 in aluminium with 14.9 percent straggling.

In Fig. 20 is shown a comparison of the range distributions of fragments of mass numbers 95, 140, 141 and 147. It is clear that the experimental method used has enabled quite precise distributions to be obtained.

Figure 19 shows the distribution in range of mass number 147 fission fragments. This was obtained by monitoring the γ ray activity from the Nd^{147} decay.

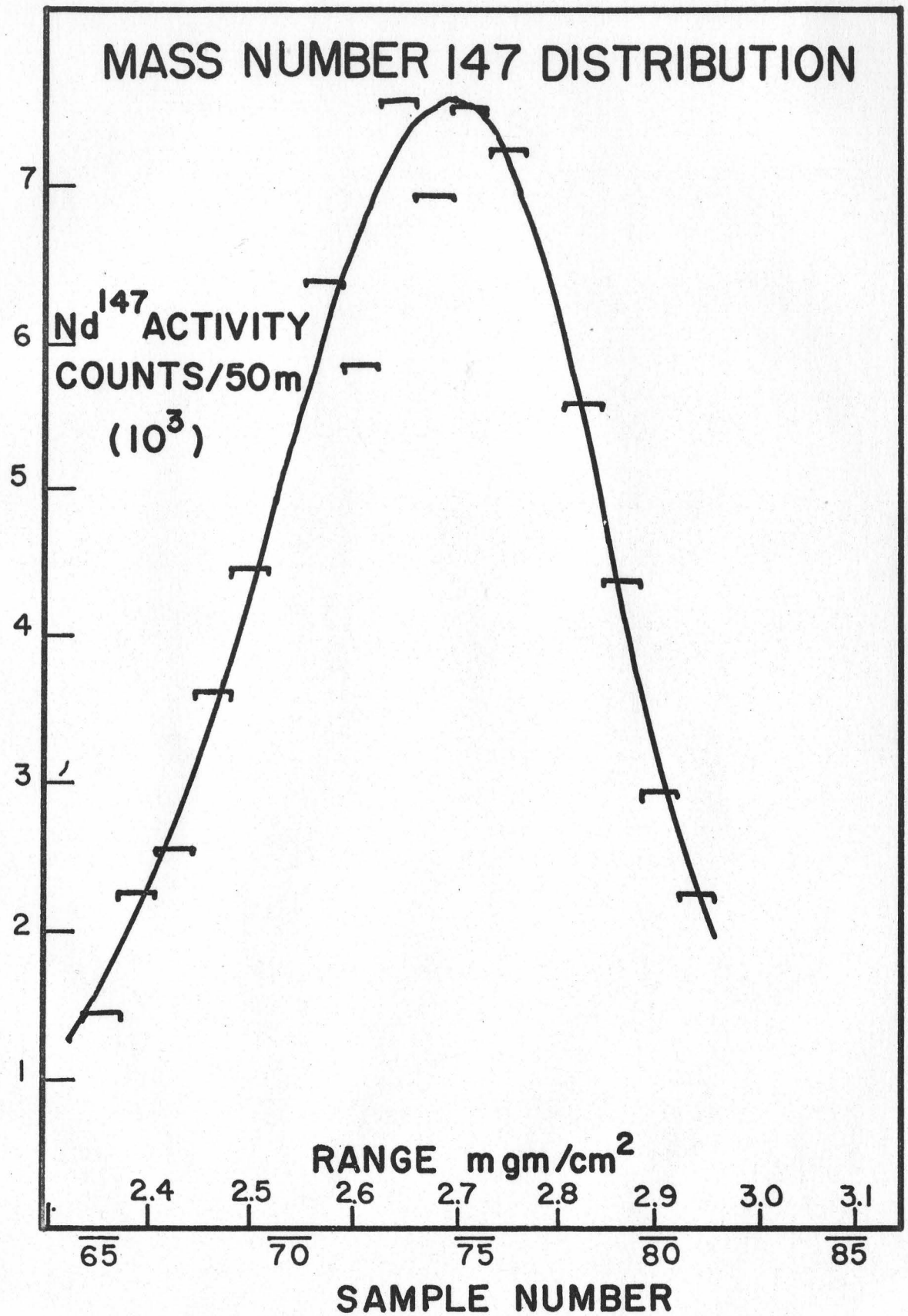
MASS NUMBER 147 DISTRIBUTION
Nd147 ACTIVITY
COUNTS/50m
(10³)
7
6
5
4
3
2
1
RANGE m gm/cm²
2.4
2.5
2.6
2.7
2.8
2.9
3.0
3.1
65
70
75
80
85
SAMPLE NUMBER

FIGURE 19

Figure 20 shows the difference in range and range straggling of fission fragments of mass numbers 95, 140, 141 and 147.

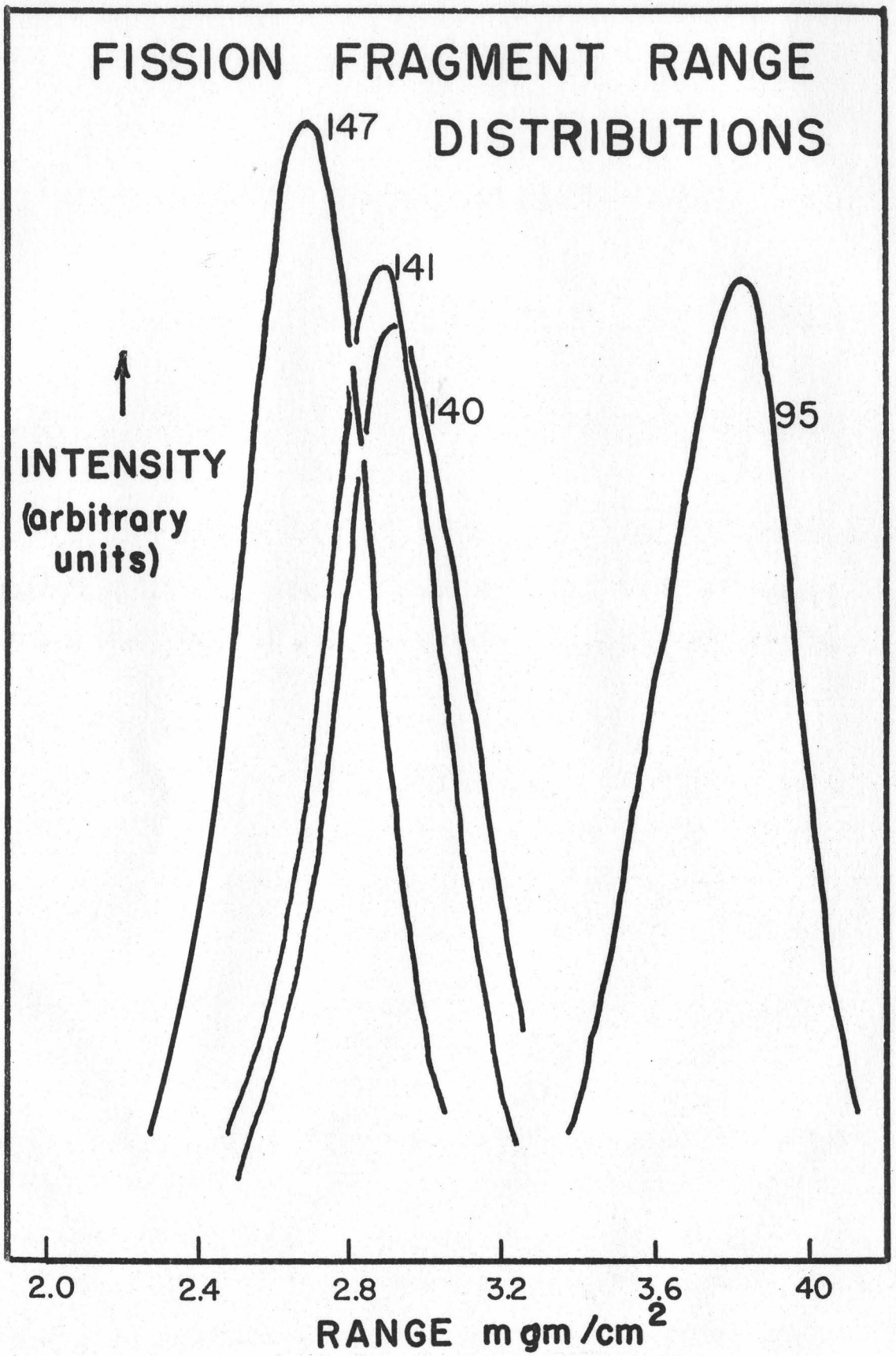
FISSION FRAGMENT RANGE DISTRIBUTIONS
147
141
140
95
INTENSITY
(arbitrary units)
2.0
2.4
2.8
3.2
3.6
40
RANGE mgm/cm²

FIGURE 20

DISCUSSION OF RESULTS

Table IV gives a comparison between the ranges and stragglings obtained in this work and those obtained by other workers. It can be seen immediately that the mean range values obtained in this work are slightly larger than those of other workers. In particular, the work of Brown and Oliver (38) should compare most accurately with this work because the same technique was used. The slightly lower values obtained for mean ranges by Brown and Oliver could probably be attributed to their use of a thicker U^{235} source (using the painting technique). The percentage stragglings obtained by Brown and Oliver - (around 17 - 18%) are very much larger than those obtained in this work. The larger stragglings obtained by Brown and Oliver could possibly be attributed again to a thick source, but are probably due to their lack of collimation in the recoil system.

The corresponding range values of Finkle et al (26) are a little smaller than those obtained in this work. However, this could be due to the fact that they measured only "extrapolated ranges" by the stacked foil technique using a rather crude arrangement.

The values of the straggling appear to increase for heavier mass fragments, at least within the experimental

TABLE IV

Comparison Data

Mass Number	Mean Range in Aluminium mgm/cm^2		% Straggling	
	This Work		This Work	
95 (Zr-Nb^{95})	3.78	3.64 (F)	11.6	
140 (Ba-La^{140})	2.94	2.75 (F) 2.82 (B)	14.6	17.5(B)
141 (Ce^{141})	2.88	2.69 (F)	13.9	
147 (Nd^{147})	2.68		14.9	
Cs^{137}		2.91 (B)		17.0(B)
Cs^{136}		2.64 (B)		17.7(B)

(F) -- Finkle et al 1951 (26)

(B) -- Brown and Oliver 1960 (38)

Note the mean ranges have an accuracy of $\sim 3\%$ which is mainly attributable to the uncertainty in the area of the catcher foil. The precision in the range measurements is about 0.5%.

error involved. This is in general agreement with Bohr's theoretical predictions (5), however, far more range values for fragments of different mass numbers would be necessary in order to check the theory explicitly.

The differential range distributions obtained in this work are believed to be far more reliable than those of Katcoff et al (7) because in this work as many as 20 individual points characterize a range distribution whereas Katcoff's work gave only about 7 or 8 points over the distribution. The stragglings observed by Katcoff for fission fragments in the mass ranges 95, 140, and 147, appear to be about ten to twenty percent lower than the corresponding straggling values obtained in this work. This is to be expected since Katcoff's straggling measurements were for fragments in air and the present measurements were in aluminium. The increase in straggling with mass of the stopping material is predicted by Bohr (5).

The assymmetry in the range distribution for fragments of mass number 95 is perhaps worth some discussion. It is possible that the assymmetry is caused by the presence of Ru^{103} in the counting samples. Ru^{103} has a half life of 41 days and a fission yield of almost 3%. It is also a gamma emitter having strong lines at 500 Kev and 611 Kev, with possibly higher energy gamma rays. Since the range distribution for mass number 95 was obtained by counting

under the γ ray peak in the region 720-760 Kev (Zr^{95}- Nb^{95} activity) it is possible that some contamination of the spectra has taken place. Ru^{103}, having a higher mass number would be expected to have a smaller range than fragments of mass number 95. This would therefore make the mass number 95 distribution somewhat screw towards the smaller range direction. This is in accordance with the observed distribution.

In conclusion it may be said that this work has tested and found satisfactory some techniques for the precise measurement of fission fragment range distributions. The distributions obtained in this work are probably the most precise yet obtained.

BIBLIOGRAPHY

1. Hahn, O. and Strassman, F., Naturwiss., 27, 11 (1939).
2. Brunton, D. C. and Hanna, G. C., Can. J. Res., 28A, 190 (1950).
3. Stein, W. E., Phys. Rev., 108, 94 (1957).
4. Lassen, N. O., Dan. Matt. Fys. Medd., 25, 11 (1949).
5. Bohr, N., Kgl. Danske Videnskab. Selskab, Matt.-Fys. Medd., 18 8 (1948).
6. Henderson, G. H., Phil. Mag., 42, 538 (1921).
7. Katcoff, S., Miskel, J. A. and Stanley, C. W., Phys. Rev., 74, 631 (1948).
8. Bohr, N., Phys. Rev., 59, 270 (1941).
9. Lamb, W. E., Phys. Rev., 58, 696 (1940).
10. Raynton, W. M. and Wilkins, T. R., Phys. Rev., 51, 818 (1937).
11. Brostøm, K. J., Bøggild, J. K. and Lauritsen, T., Phys. Rev., 58, 651 (1940).
12. Bøggild, J. K., Brostrøm, K. J. and Lauritsen, T., Phys. Rev., 59, 275 (1941).
13. Lark-Horovitz, K. and Miller, W. A., Phys. Rev., 59, 941 (1941).
14. Demers, P., Phys. Rev., 70, 974 (1946).
15. Silk, E. C. H. and Barnes, R. S., Phil. Mag., 4, 970 (1959).
16. Noggle, T. S. and Stiegler, J. O., J. Appl. Phys. 31, 2199 (1960).
17. Bøggild, J. K., Arrøe, O. H. and Sigurgeirsson, T., Phys. Rev., 71, 281 (1947).
18. McMillan, E., Phys. Rev., 57, 510 (1939).

19. Joliot, F., Comptes rendus., 218, 488 (1944).

20. Segrè, E. and Wiegand, C., Phys. Rev., 70, 808 (1946).

21. Sugarman, N., J. Chem. Phys., 15, 544 (1947).

22. Suzor, F., Comptes rendus, 224, 1155 (1947).

23. Suzor, F., Comptes rendus, 226, 1081 (1948).

24. Freedman, M. S., Metcalf, R. P. and Sugarman, N., NNES, Div IV, 9, Book 1 paper 44 (1951).

25. Finkle, B., Hoagland, E. J., Katcoff, S. and Sugarman, N., NNES, Div IV, 9, Book 1 paper 45 (1951).

26. Finkle, B., Hoagland, E. J., Katcoff, S. and Sugarman, N., NNES, Div IV, 9, Book 1 paper 46 (1951).

27. Douthett, E. M. and Templeton, D. H., Phys. Rev., 94, 128(1954).

28. Alexander, J. M. and Gazdik, M. F., Phys. Rev., 120, 874 (1960).

29. Niday, J. B., Phys. Rev., 121, 1471 (1961).

30. Joliot, F., Comptes rendus, 208, 341 (1939).

31. Corson, D. R. and Thornton, R. L., Phys. Rev., 55, 509 (1939).

32. Anderson, H. L., Booth, E. T., Dunning, D. R., Fermi, E., Glasoe, G. W. and Slack, F. G., Phys. Rev., 55, 512 (1939).

33. Booth, E. T., Dunning, J. R. and Glasoe, G. N., Phys. Rev., 55, 982 (1939).

34. Joliot, F., Comptes rendus, 208, 647 (1939).

35. Bøggild, J. K., Minnhagen, L. and Nielsen, O. B., Phys. Rev., 76, 988 (1949).

36. Good, W. M. and Wollan E. O., Phys. Rev., 101, 249 (1956).

37. Smith, E. R. and Frank, P. W., WAPD-TM-198 (AEC) (1959).

38. Brown, F. and Oliver, B. H., Third Symposium on Nuclear and Radiochemistry, Chalk River, Sept. 1960, paper 21.

39. Povelites, J. G., P/664, Geneva Conference 1958.

40. Glover, K. M., J. Nuc. Energy, 1, 214 (1955).

41. Seaborg, G. T., Katz, J. J. and Manning, W. M., "The Transuranium Elements" Vol. II 1204, McGraw-Hill, N.Y., (1949).

42. Wilson, C. R. and Lanzer, A., Nucleonics, 11, No. 8, 48 (1953).

43. Brodsky, A., Fagg, L. W. and Hanscome, T. D., Health Physics, 1, 189 (1958).

44. Miskel, J. A., Private Communication, UCRL Livermore Laboratories, California, 1960.

45. Holland, L., "Vacuum Deposition of Thin Films" Chapman & Hall, London, (1956).

46. Carswell, D. J. and Milstead, J., J. Nuc. Energy, 4, 51 (1957).

47. Güntherschulze, A. and Betz, H., "Elektolytkondensatoren", M. Krayn, Berlin (1937).

48. Strohmaier, K. Z. Naturforschg., 6a, 508 (1951).

49. Davies, J. A., Friesen, J. and McIntyre, J. D., Can. J. Chem., 33, 1526 (1961).

50. Berman, A., Bleiberg, T. and Yeniscavich, I., WAPD-T-1125 (AEC), (1960).